Androgen regulated processing of the oncomir MiR-27a, which targets Prohibitin in prostate cancer

Authors: Claire E. Fletcher[1], D. Alwyn Dart[1], Ailsa Sita-Lumsden[1], Helen Cheng[2], Paul S. Rennie[2], Charlotte L. Bevan[1*]

Affiliations: [1]Androgen Signalling Laboratory, Department of Surgery and Cancer, Imperial College London, London W12 0NN, UK. [2]Vancouver Prostate Centre, Vancouver BC V6H 326, Canada.

***Contact Information for Corresponding Author:** Charlotte Bevan, Department of Surgery and Cancer, Imperial College London, Hammersmith Hospital Campus, London W12 0NN, UK. Tel: +44-207-5941685. Fax: +44-208-3835830, Email: charlotte.bevan@imperial.ac.uk.

Abstract

MicroRNAs (miRs) play an important role in the development of many complex human diseases and may have tumour suppressor or oncogenic (oncomir) properties. Prostate cancer is initially an androgen-driven disease, and androgen receptor (AR) remains a key driver of growth even in castration-resistant tumours. However, AR-mediated oncomiR pathways remain to be elucidated. We demonstrate that miR-27a is an androgen-regulated oncomir in prostate cancer, acting via targetting the tumour suppressor and AR corepressor, Prohibitin (PHB). Increasing miR-27a expression results in reduced PHB mRNA and protein levels, and increased expression of AR target genes and prostate cancer cell growth. This involves a novel mechanism for androgen-mediated miR regulation, whereby AR induces a transient increase in miR-23a27a24-2 transcription, but more significantly accelerates processing of the primiR-23a27a24-2 cluster. Androgens therefore regulate miR-27a expression both transcriptionally (via AR binding to the cluster promoter) and post-transcriptionally (accelerating primiR processing to the mature form). We further show that a miR-27a anti-sense oligonucleotide, by opposing the effects of mir-27a, has therapeutic potential in prostate cancer.

Introduction

Prostate cancer (PCa) is the most prevalent non-cutaneous malignancy in Western males (1). Initially, growth of prostate tumours is dependent on circulating androgens, which exert their growth-stimulatory effects through association with the androgen receptor (AR) (2). AR is a ligand-dependent transcription factor, activation of which by androgens initiates target gene transactivation resulting in PCa cell proliferation. This involves dimerization and recruitment to androgen response elements (AREs) of coactivators and/or corepressors (3-7), whose roles in PCa remain poorly understood. MicroRNAs (miRs), which have been shown to function as oncogenes and tumour suppressors in multiple cancers (8-11), may play an important role in PCa through targeting coregulators of AR and targets involved in growth response. Further, several miRs demonstrate androgen regulation, although the mechanisms surrounding such regulation remain to be elucidated. In this study, we demonstrate inhibition of the AR corepressor, Prohibitin (PHB), by hsa-miR-27a (henceforth referred to as miR-27a) in PCa, and identify a mechanism by which AR mediates post-transcriptional miR-27a maturation. Importantly, as well as being an AR corepressor, PHB is an AR target protein, downregulation of which promotes cell growth, implying a tumour suppressor function (12-14). How much of this relates to its corepressor role is not clear. Thus, miRs that inhibit AR targets and/or coregulators to modulate androgen response may represent novel targets for PCa therapeutics.

PHB is an evolutionarily conserved protein with multiple cellular functions (15-22) that negatively regulates AR activity and androgen-stimulated growth of PCa cells (13). A reduction in PHB either by androgens or RNAi-mediated knockdown resulted in increased AR activity and enhanced growth of prostate xenografts (LNCaP) (14). Our initial observation that AR downregulates PHB was followed by evidence that this occurs at least partly at the level of transcription. Indeed, PHB regulation may involve several mechanisms,

such as genomic effects at the PHB promoter or post-translational modifications. A more recent hypothesis suggests a role for miR association with PHB 3'UTR in regulation of PHB (23). However, the precise mechanism of androgen or AR-mediated downregulation of genes such as PHB is unknown. Interestingly, we found that the optimum RNAi oligo for PHB knockdown shared considerable sequence similarity to a previously published oncomiR targeting PHB-3'UTR – namely miR-27a (23). PHB has a large, highly conserved 3'UTR, with several putative miR binding sites, indicating that miRs may be heavily involved in its regulation.

MiRs are 19-25nt non-coding RNAs that regulate target gene expression through translational inhibition or transcript degradation (24), regulating a wealth of biological processes including tumourigenesis (25). Further, approximately 50% of miR genes are in cancer-associated genomic regions or in fragile sites (26). It is, therefore, conceivable that miRs have a significant effect on cell physiology and that common single-nucleotide polymorphisms (SNPs) within key miR target sites could contribute significantly to an individual's risk of developing complex diseases. Functional studies have also established that individual miRs can act as oncogenes (oncomiRs) or tumour supressors (8), and although targets of many miRs remain to be elucidated, some have been shown to repress well-known oncogenes or tumour supressors. For example, miR-15/16 inhibit the anti-apoptotic factor BCL2, an anti-apoptotic factor (27), while the let-7 family of miRs target the Ras oncogene (28). Thus, miR aberrations may be involved in prostate oncogenesis and development of castration resistant PCa (CRPC) (10, 29, 30). Several studies have revealed distinct miR signatures in prostate tumours compared to benign samples (11, 31, 32).

MiR-27a is encoded in an intergenic cluster with miR-23a and miR-24-2 located on chromosome 19p13.1. The ~2159nt primary transcript is transcribed from a promoter region located between -603 and +36nt (33). The -530 to -410 promoter portion contains two GC-

rich domains and is thought to be the location for transcription factor binding (34, 35). Expression of the miR23a27a24-2 cluster is altered in many cancers, including leukemia (36, 37), breast cancer (38), colorectal cancer (39), hepatocellular carcinoma (40), ovarian cancer (41) and PCa (11, 32). Upregulation of this cluster has been shown to reduce tumour suppressive effects of TGFβ in human hepatocellular carcinoma cells (40); conversely, it induced apoptosis in human embryonic kidney cells (42). The diverse effects of this cluster suggest context-dependent activities, warranting investigation into the individual molecular functions of the cluster members and identification of targets, especially given evidence of differential regulation of miR-23a27a24-2 cluster members. For example, downregulation of miR-27a has been observed independently of miR-23a and miR-24-2 (43), and it is likely that both transcriptional and post-transcriptional mechanisms may be involved in cluster regulation.

As miR-27a has been proposed to function as an oncomiR in gastric cancer through downregulation of PHB (23) and given the androgen-mediated downregulation of PHB and the role of PHB in AR repression, we hypothesised that the AR itself may modulate levels of miR-27a thus downregulating its own repressor (PHB) in a 'positive feedback loop'. MiR-27a targeting of PHB could play an important role in PCa progression in several ways; through reducing AR repression and by downregulating other repressive roles of PHB, resulting in maintenance of oncogenic phenotype.

Results

Androgen Regulation of PHB Occurs Largely at the 3'UTR

In the LNCaP PCa cell line, androgen treatment reduces PHB levels by approximately 50% (13). However, PHB promoter activity shows a maximum reduction of only 25% following AR activation (Fig S1), therefore we hypothesised that androgen regulation of PHB may occur at the 3'UTR. PHB-3'UTR sequence was fused to a luciferase reporter (Fig S1B+C) and HeLa cells were transiently transfected with this reporter and AR expression vector. Luciferase activity was reduced by approximately 25% upon androgen treatment (Fig 1A), supporting the hypothesis that androgens downregulate PHB via the 3'UTR. This is mediated by AR, since AR silencing (using a doxycycline-inducible system (44)), resulted in increased PHB-3'UTR levels, which was not observed using scrambled shRNA (Fig 1B). In further support of a role for the 3'UTR in androgen regulation of PHB, when another PCa cell line, PC3wtAR cells, were treated with androgen and primer-specific qRT-PCR performed for either the PHB coding region or PHB-3'UTR, reduction in PHB 3'UTR was 85% compared to 45% for the coding region (Fig 1C). Finally, anti-androgen treatment abrogated the effects of MB at the endogenous PHB-3'UTR: whilst PHB-3'UTR PCR product levels were drastically reduced following androgen treatment of LNCaP cells (Fig 1D), addition of Bicalutamide (Bic) reversed this effect. These data suggest that androgen exerts inhibitory effects on PHB via the 3'UTR.

PHB is a Target of MiR-27a in PCa Cells

Putative miR binding sites in the PHB-3'UTR were mapped (microRNA.org) (Fig S2) and showed eight groupings within the 3'UTR, including a binding site for miR-27a, of interest

due to its reported role as an oncomiR targeting PHB in gastric cancer (23). High sequence complementarity exists between PHB 3'UTR and the miR-27a seed region (Fig 2A). To confirm that PHB-3'UTR contains *bona fide* miR-27a target sequences, the PHB 3'UTR reporter vector was transfected into HeLa cells with expression vectors for AR and miR-27a mimic (p2TetR-miR-27a: since HeLa cells lack Tet repressor, doxycycline (dox) was not required to derepress miR-27a mimic expression). A mutant form of the PHB-3'UTR was also tested, carrying two nucleotide changes in the putative miR-27a seed region (Fig 2A). Whilst addition of miR-27a mimic resulted in 60% reduction in PHB-3'UTR activity, it did not significantly alter activity of the mutated reporter (Fig 2B), demonstrating that PHB-3'UTR is a direct target of miR-27a via this site. To assess whether miR-27a can reduce levels of endogenous PHB in PCa cells, LNCaP cells expressing miR-27a under dox control were created (LNCaP/TR2/miR-27a). Induction of exogenous miR-27a mimic resulted in a considerable reduction in PHB protein levels 24h post dox treatment compared to non-induced cells, with optimal 90% reduction in PHB protein observed following 0.1μM dox treatment (Fig 2C). To address the physiological relationship between endogenous miR-27a and PHB in PCa, PHB protein and miR-27a levels were assessed by Western blotting and qRT-PCR respectively in a panel of representative human cell line models. A significant inverse correlation between PHB protein levels and miR-27a levels was found, with a Pearson correlation coefficient of -0.881. This suggests that levels of PHB and miR-27a are closely linked in PCa, supporting PHB as an endogenous target of miR-27a in this disease.

To investigate whether repression of PHB-3'UTR is via translational repression or transcript degradation, levels of PHB-3'UTR were assessed by qRT-PCR in LNCaP/TR2/miR-27a cells induced with dox. Increasing miR-27a levels resulted in up to 70% reduction in PHB-3'UTR levels (representing the complete mRNA) compared to untreated cells (Fig 2E). This suggests that miR-27a induces degradation of the PHB

transcript following binding to the PHB-3'UTR. To confirm whether these effects on PHB are specifically attributable to miR-27a, miR-27a anti-sense oligonucleotide (ASO) was transfected into LNCaP cells in the presence or absence of miR-27a. In agreement with Figure 2C, miR-27a significantly reduced PHB protein levels by up to 70% (Fig 2F). Addition of ASO rescued miR-27a-mediated PHB loss, while transfection of ASO alone increased PHB protein levels approximately 2.6-fold. Next, the impact of ASO introduction on PHB-3'UTR activity was assessed in HeLa cells. MiR-27a reduced PHB-3'UTR activity by approximately 60% and this was restored to empty vector-transfected control levels upon addition of 1-10μg ASO, in a dose-dependent manner (Fig 2G). Further, transfection of the ASO into LNCaP cells increased PHB-3'UTR transcript levels compared to untransfected or scrambled control-transfected cells, presumably by acting on endogenous miR-27a (Fig 2H). Taken together, these data confirm that miR-27a targets PHB-3'UTR in PCa cells through seed region binding, leading to transcript disruption and/or translational inhibition and loss of PHB protein, which can be abrogated through addition of miR-27a ASO.

MiR-27a Overexpression Results in Increased Expression of Androgen-Regulated Genes and Increases PCa Cell Growth

Since PHB is an AR corepressor, the impact of PHB reduction on expression of *PSA* and *TMPRSS2* (well-characterised AR-responsive genes) was examined by qRT-PCR after dox induction of LNCaP/TR2/p2TetR-miR-27a cells. PSA and TMPRSS2 mRNA levels were increased up to 3.2-fold following induction of exogenous miR-27a expression (Fig 3A). To investigate effects of miR-27a on LNCaP PCa cell growth, the same cells were treated with 10nM MB ± dox, and cell number assayed at intervals up to 6 days. Androgen treatment increased cell growth 1.5-fold compared to vehicle-treated control cells at 6 days (Fig 3B). Exogenous expression of miR-27a mimic (Dox + MB) resulted in a significantly greater, 1.7-fold increase in cell growth compared to vehicle-treated control cells at 6 days. Induction of

miR-27a mimic in androgen-depleted medium did not increase cell growth, suggesting that miR-27a plays a role in androgen-dependent growth. To investigate whether the growth-stimulatory effects of miR-27a could be specifically attributed to targeting of PHB, a plasmid expressing tagged PHB (pcDNA4/TO-GFP-PHB) was introduced into the above system. It was found that increasing PHB resulted in decreased cell growth even in the presence of exogenous miR-27a (Fig 3B: note that non-normalised data is shown on the right to illustrate the effect of miR-27a on growth in the presence of androgen), i.e. PHB can indeed suppress miR-27a-mediated growth stimulation. Induction of miR-27a expression and GFP-PHB transfection did not alter cell growth in the absence of MB (Fig S3). In a reciprocal experiment, stable LNCaP/GFP-PHB cells were transfected with miR-27a or a negative control oligo and treated with MB ± dox to induce GFP-PHB expression (Fig 3D). In agreement with Fig 3B, it was found that miR-27a overexpression in the absence of exogenous PHB led to a significant 80% increase in androgen-induced cell growth. In contrast, upon induction of GFP-PHB expression, no significant difference was observed between miR-27a-transfected and non-transfected cells, suggesting that overexpression of PHB is able to compensate for the growth increase induced by miR-27a of PHB 3'UTR. It should be noted that the exogenous PHB lacks the 3'-UTR hence would not be targeted by miR-27a. These data suggest that the growth-stimulatory effects of miR-27a in PCa cells are largely attributable to miR-27a targeting of PHB, without ruling out a contribution of other miR-27a-regulated transcripts.

As miR-27a increased PCa cell growth, we hypothesised that miR-27a ASO may inhibit proliferation. In support of this, whilst androgen treatment of LNCaP cells transfected with scrambled ASO gave a three-fold increase in cell number after 6 days, the increase was reduced to 1.5-fold in cells transfected with miR-27a ASO in the presence of androgen (Fig 3E). Together these data indicate that miR-27a targeting of PHB increases AR activity in PCa

cells through loss of PHB corepressive activity, and that manipulation of miR-27a alters PCa cell growth.

The MiR-23a27a24-2 Cluster is Regulated by Androgen and AR in PCa Cells

Since both androgen signalling and miR-27a downregulate PHB, we investigated whether miR-27a is androgen regulated. LNCaP cells were treated with 10nM MB or ethanol for 0-24h and endogenous mature miR-27a assayed by qRT-PCR. MiR-27a expression increased by >2-fold after 4h and by 2.9-fold after 24h in LNCaP cells treated with MB, compared to time zero ($P \leq 0.05$, Fig 4A). This is consistent with the magnitude of fold-increases reported in microarray analysis of AR-regulated miRs in PCa (11).

As miR-27a is polycistronically transcribed (Fig 4B), we next examined whether miR-27a cluster partners, miR-23a and miR-24-2 demonstrate androgen regulation. qRT-PCR was performed for mature miRs 27a, 23a and 24-2 following treatment of LNCaP cells with androgen and an anti-androgen (Bic). All three miRs were significantly increased following MB treatment, but decreased to near-vehicle control levels upon addition of anti-androgen. (Fig 4C). The extent of regulation varied for the three cluster members, with miR-27a demonstrating a greater response to MB (5-fold increased expression) compared to miR-23a and miR-24 (3.8-fold and 2-fold respectively). These changes in mature miR levels are confirmed as AR-specific as they can be negated by anti-androgen treatment. To confirm that androgen regulation of miR-27a is not a cell line-specific effect, PC3wtAR cells (45) were treated with MB ± Bic for 24 hours followed by Northern blotting of total RNA (Fig 4D). Again, androgen treatment increased miR-27a levels in a dose-dependent manner, and this was abrogated by anti-androgen treatment.

AR Associates with the Proximal MiR23a27a24-2 Promoter in PCa Cells in Response to Androgen Treatment to Enhance Transcription and also acts to Enhance Drosha-Mediated PrimiR-23a27a24-2 Processing

The observation that all three members of the miR-23a27a24-2 cluster demonstrate androgen regulation suggested this may be mediated through association of liganded AR with AREs within the cluster promoter. We used the ALGGEN algorithm (http://alggen.lsi.upc.es/) to predict putative AREs or half-sites within the miR-23a27a24-2 promoter. Two predicted AREs were identified within 300bp 5' of the miR-23a27a24-2 transcription start site (Fig S3A). To assess whether the proximal miR promoter can confer androgen responsiveness upon a luciferase reporter gene, indicative of primiR transcription, an 800bp proximal portion (-726 to -23) and a 1.1kb distal portion (-2982 to -1942) of the miR cluster promoter were inserted upstream of the *luc2* gene in the pGL4.18 vector and transfected intoos-1 cells alongside AR expression vector. Activity of the proximal fragment was increased five-fold following androgen treatment compared to vehicle-treated cells (Fig 5A), however miR distal promoter activity was unchanged, suggesting this region is not androgen responsive. To assess whether liganded AR can directly associate with the proximal miR cluster promoter, ChIP analysis was performed on LNCaP cells following treatment with MB or vehicle for 0-2 hours, using primers to amplify a 352bp portion of the proximal miR cluster promoter (Fig S4A). AR was significantly enriched by approximately 2.5-fold on the proximal miR cluster promoter in LNCaP cells after 30 minutes of androgen treatment compared to vehicle-treated cells (Fig 5B). However, association appears to be transient, as enrichment was reduced to basal levels after 60 and 120min of androgen treatment. The well-defined androgen-regulated *PSA* gene promoter was used as a positive control throughout ChIP experiments (Fig S4B-E). The above data suggest that AR is able to associate with the miR-23a27a24-2 promoter in response to androgen to initiate transcription of the cluster, albeit in a transient manner.

As miR-27a and its cluster partners are polycistronically transcribed and all demonstrate androgen regulation, we wished to confirm whether AR association with the miR-23a27a24-2 promoter leads to androgen-dependent transcription of the entire endogenous miR-23a27a24-2 cluster. LNCaP cells were treated with MB for 0-24 hours and qRT-PCR was performed using primers designed to amplify miR-23a27a24-2 primary transcript (primiR-23a27a24-2). PrimiR levels were increased 7-fold 1 hour post-androgen treatment, whereafter primiR levels declined until, after 24 hours of androgen treatment, primiR levels were similar to vehicle-treated cells (Fig 5C). MB-mediated AR activation across this time frame was confirmed by increased *PSA* expression (Fig S5). Together with Fig 4A, Fig 5C suggests that an initial peak in primiR levels is translated into later increase in mature miR levels, with the possibility that androgen treatment acts not only at the miR cluster promoter, but also to enhance pri-mir or pre-mir turnover. In corroboration of this, examination of primiR-23a27a24-2 levels following AR silencing revealed primiR accumulation, rather than loss, in PCa cells following induction of AR shRNA, whereas induction of scrambled shRNA had no effect on primiR levels (Fig 5D). These data indicate a further role for liganded AR in enhancing primiR/premiR processing, as AR-mediated miR promoter activation could not explain the observed decrease in primiR transcript levels following AR silencing. To investigate the ability of AR to enhance Drosha-mediated primiR-23a27a24-2 processing, we generated a reporter vector in which the genomic miR-23a27a24-2 sequence is located 5' of the *luc2p* gene, under the control of a CMV promoter. Transcription yields primiR-23a27a24-2 transcript linked to the luc2p transcript. Drosha-mediated cleavage of the primiR disrupts the transcript, resulting in loss of luciferase activity - thus Drosha activity is inversely correlated with luciferase activity. This system has been shown to be a sensitive assay for Drosha-mediated cleavage of a specific primiR species in previous studies (46-48). The primiR-23a27a24-2 Drosha cleavage reporter was transfected

into Cos-1 cells alongside AR and increasing doses of MB and Bic. Luciferase activity was significantly reduced in the presence of MB with reference to vehicle-treated cells, suggesting that androgen treatment increased Drosha cleavage of primiR-23a27a24-2. Addition of Bic to this system was able to abrogate the effect of androgen treatment on Drosha activity, confirming that liganded AR is able to specifically enhance Drosha processing of primiR-23a27a24-2. These effects were not observed in the absence of AR (Fig S6A) or upon transfection of the empty CMV-GL4 plasmid (Fig S6B).

AR Regulation of MiR-27a Occurs During Post-Transcriptional Processing of PrimiR to PremiR

To confirm that androgen regulation of miR-27a occurs post-transcriptionally, we investigated the ability of miR-27a and its cluster partners to accumulate in the absence of active transcription through treatment of LNCaP cells with the transcription-blocking agent, Actinomycin D (ActD), ± androgen. We observed that after 6 hours treatment of cells with ActD and androgen, primiR levels were increased 6-fold due to the presence of MB prior to degradation of transcripts (Fig 6Ai). However, at later time points, primiR levels were drastically reduced due to transcriptional blocking and transcript degradation (Fig 6Ai). Of note: transcription of another androgen-regulated gene, KLK2, showed a similar decrease at 24 and 48h post actinomycin treatment but without the initial peak at 6h, presumably due to different dynamics of AR regulation of this gene (Fig S7). In contrast to these primary transcripts, mature miR-27a levels were increased 6-fold at 48h post treatment (Fig 6Ai), showing a similar pattern of expression to that observed following androgen treatment in the absence of ActD (see Fig 4A). As expected, miR-27a levels were unchanged in the presence of ActD and ethanol (Fig 6Aii), likely due to lack of activated transcription and miR stability. L19 mRNA levels were significantly reduced by ActD treatment in the presence or absence of androgen, confirming transcriptional inactivation by ActD (Fig 6Aiii). These data suggest

that active transcription is not required to increase miR-27a levels following androgen treatment, and in combination with results shown in Fig 5E support the hypothesis that active androgen regulation of the miR cluster occurs during primiR to premiR processing. In confirmation of this, miR23a and miR24-2 are also increased in the presence of androgen, but not ethanol, following transcriptional inactivation (Fig 6B and 6C respectively). In contrast, miR-182, which we previously found to be unresponsive to androgen (data not shown), shows no difference in expression between vehicle and androgen treated cells following addition of ActD (Fig 6D). In addition, figures 6E and F show that, while primiR-23a27a24-2 levels are reduced following 24h MB treatment (Fig 6E), mature miR-27a levels show the opposite, demonstrating a near 1.8-fold increase (Fig 6F). Treatment with the antiandrogen Bic abrogated both MB-induced primiR decrease and miR-27a increase. Addition of Bic alone did not alter miR-27a levels but led to a small increase in primiR levels, presumably due to stabilisation of the primiR. These data demonstrate that androgen treatment alters the equilibrium between primiR-23a27a24-2 and mature miR-27a, favouring accelerated miR-27a production by enhancing Drosha-mediated primiR cleavage. To confirm that androgen-enhanced post-transcriptional processing of primiR-23a27a24-2 requires AR, levels of mature miR-27a were assessed in LNCaP cells following dox-mediated induction of AR shRNA. Levels of miR-27a were 50% lower in PCa cells following AR silencing in the presence of androgen with reference to androgen only-treated cells (Fig 6F). This indicates that AR is required for androgen-induced primiR-23a27a24-2 to premiR-23a27a24-2 processing.

Together these data indicate that androgen regulation of the miR-23a27a24-2 cluster occurs via two distinct processes. Initial regulation is at the level of transcription through transient association of AR with the miR cluster promoter, resulting in increased levels of the primiR. Additionally, androgens then promote Drosha-mediated primiR to premiR processing resulting in increased mature mir-27a (and other cluster partners). Data presented here also

suggest that there may exist a mechanism of androgen-mediated regulation that is specific to miR-27a, as miR-27a shows a greater androgen response than either miR-23a or miR-24-2.

Discussion

Previous studies suggested that downregulation of PHB by AR is a key step in cell cycle initiation in androgen-dependent cells, and PHB may thus play an important role in PCa (14). We found that PHB regulation by androgens is largely mediated by miRs, specifically miR-27a. MiRs can act as oncogenes and tumour suppressors in a multitude of cancers. It is our hypothesis that oncomiRs can act by targetting important components of the androgen signalling pathway in PCa, and such oncomiRs may themselves be androgen regulated. This would result in a complex regulatory feedback loop that permits fine-tuning of AR activity. In gastric adenocarcinoma cells, inhibiting miR-27a was shown to inhibit growth, suggesting that it can act as an oncogene (23). We show here that miR-27a is subject to androgen regulation and demonstrate the direct consequences of miR-27a activity, and suppression thereof, on PHB expression, PCa cell growth and AR target gene expression. Further, we identify a novel mechanism for post-transcriptional modulation of miR biogenesis by AR.

The PHB-3'UTR contains one predicted miR-27a binding site approximately 100bp 3' of the end of the coding region, which is highly conserved. This UTR conferred susceptibility for androgen-mediated downregulation to a luciferase reporter gene, suggesting that an androgen regulated factor associates with PHB-3'UTR to reduce its activity (Figure 1). AR silencing/inhibition increased levels of PHB transcript, confirming the requirement for AR in regulation of PHB 3'UTR. A candidate intermediary factor was miR-27a, which we confirmed reduced PHB levels via specific binding to the 3'-UTR (Fig 2). The dominant

mechanism appears to be transcript degradation, rather than translational inhibition. Interestingly, PHB-3'UTR mutations have been reported in a number of breast cancer cell lines, including BT-20, SK-BR-3 and MCF7 (49), raising the possibility that mutations may occur in miR binding sites. Indeed, Sato *et al* demonstrated mutation of PHB in sporadic breast cancer (50) and Jakubowska *et al* have identified a C>T polymorphism in the 3'UTR of PHB as a breast cancer risk modifier in a Polish cohort carrying a *BRCA1* mutation (51). *In silico* analysis performed on PHB 3'UTR mutations identified in breast cancer cell lines (49) has shown mutations in putative binding sites for several miRs. However, it is as yet unknown whether these miRs target PHB *in vivo* and whether they have roles in cancer; no mutations have yet been identified in the miR-27a binding sequence.

Functional consequences of miR-27a manipulation in PCa cells include increased expression of androgen regulated genes, *PSA* and *TMPRSS2*, and increased androgen-dependent growth. Conversely, the miR-27a ASO significantly reduced growth in the presence of androgen (Figure 3). In this context, it is noteworthy that *Wee-1* and *Myt-1* (important regulators of cyclin B and cdc2, which, like PHB, have roles in cell cycle progression) both contain potential miR-27a complementary sites in their 3'UTRs and have been demonstrated to be *bone fide* targets (38). Further, it has been demonstrated in breast cancer that miR-27a targets ZBTB10, a repressor of the Sp family of transcription factors that have been implicated in carcinogenesis in breast cancer (38), and this may indirectly effect ERα levels (52). The observed increase in PARP cleavage upon miR-27a ASO transfection and decrease in anti-apoptotic survivin and anti-angiogenic VEGF and VEGFR1 (38) demonstrates the potential of miR-27a to function as an oncomiR *in vivo* by targeting several tumour suppressor proteins. An additional miR-27a target is the tumour suppressor FOXO1, which has important roles in cell cycle regulation and initiation of apoptosis (53). Similarly to PHB, it has been shown to be hormonally regulated and is downregulated in several cancers,

including endometrial carcinoma and ovarian cancer (54). These observations suggest that miR-27a targets proteins with important cell cycle regulatory roles, and, at least in PCa, androgen-mediated upregulation of miR-27a may be required to downregulate cell cycle inhibitors for cell cycle initiation and cell growth. This highlights the potential 'oncomiR' function of miR-27a.

The multitude of potential miR-27a targets, several of which are also tumour suppressors, make it difficult to ascertain the relative contribution of miR-27a-targetting of a particular mRNA to observed phenotypic changes. An additional complicating factor is that miRs often act as "tuning agents". In this model, miRs can function as rheostats to dampen protein levels to a more desirable level whilst still permitting the target protein to carry out essential functions in the cells. The combinatorial effects of low-level downregulation of multiple miR targets likely accounts for observed physiological effects following altered miR expression, rather than high efficiency targeting of a small number of mRNAs. Thus it cannot be discounted that the effects of miR-27a manipulation outlined here are due to low-level repression of several mRNA species. An argument for the key role of PHB is that we demonstrated that adding back PHB to cells with increased miR-27a resulted in inhibition of miR-27a-stimulated growth (Fig 3), indicating that here miR-27a is exerting its effects largely via PHB. However the suppression was not total. This could be a dosage effect but another likely explanation is that miR-27a suppression of other targets also contributes to the observed growth stimulation.

We found that androgen regulation of miR-27a occurs via several mechanisms. Levels of the cluster primary transcript, primiR-23a27a24-2, initially increased with androgen treatment but soon after decreased, suggesting that androgen acts both to rapidly and directly increase primiR levels and also increase the rate of primiR or premiR processing thus depleting the primiR (Figures 5 and 6). This hypothesis is supported by the steady increase in

mature miR-27a following androgen addition. The mechanism of androgen regulation, therefore, appears not to be primarily stabilisation of the mature miR. As no evidence exists for independent primiR expression within the miR-23a27a24-2 cluster (unlike the miR-23b27b24-1 cluster) and no internal poly(A) binding sites have been identified (43), and given the observation that both cluster partners, miR-23a and miR-24-2, demonstrate androgen regulation, we initially hypothesised that such regulation occurs at the level of transcription from the miR promoter and/or processing of the primary transcript. However, since the three miRs of the cluster show differing degrees of androgen regulation (Figure 4), it is possible that other unique regulation mechanisms exist, acting after primiR cleavage.

When assessing miR cluster promoter activity we found that the proximal 700bp conferred androgen responsiveness to a reporter, and within this saw androgen-dependent AR association with the proximal –366 to –24 region (containing two predicted AREs) (Figure 5). However, these moderate effects may not entirely explain the rapid accumulation of primary transcript 1h after MB treatment. AR may associate with additional regions or may require other factor(s) to associate efficiently with the miR promoter. Taken together, these data results indicate that transient association of AR with the miR-23a27a24-2 promoter results in a pulse of transcription of the miR cluster shortly after androgen treatment. However, primiR levels were increased following AR silencing (Fig 5D) or anti-androgen treatment (Fig 6E), an apparently paradoxical result. We showed using a Drosha cleavage reporter vector specific for the miR-23a27a24-2 cluster that androgens promote the cleavage of the primiR, which explains the increase in primiR upon AR silencing/inhibition, since blocking this processing would result in accumulation of the primiR. Thus it seems that AR also acts post-transcriptionally during miR biogenesis to increase miR-27a levels, supported by the fact that miR-27a, 23a and 24-2 accumulate in the absence of transcription following addition of androgens (Fig 6). While we have demonstrated that AR acts during Drosha-

mediated primiR processing, the possibility that AR also acts to enhance Exportin 5-mediated primiR export, or to accelerate premiR processing by Dicer, cannot be entirely discounted. Work is ongoing to elucidate exactly where AR exerts its effects on miR-23a27a24-2 processing and if this mechanism is unique to this cluster.

This report proposes a novel mechanism for androgen regulation of oncomiR-27a and its growth suppressor target, PHB, in PCa, summarised in Figure 7. Androgen signalling results in a reduction in transcription of the PHB gene as shown previously (12). Additionally, androgen treatment leads to upregulation of miR-27a, through enhanced cluster transcription and increased primiR processing. MiR-27a then associates with the PHB-3'UTR, resulting in transcript disruption and translational inhibition. These effects may be combinatorial and result in loss of PHB activity with a subsequent increase in AR activity and cell growth. As miR-27a ASO has been shown to increase PHB protein levels and reduce androgen-dependent PCa cell growth, miR-27a ASO may represent a novel therapeutic for the treatment of PCa.

In conclusion, we have identified complex, multi-level regulation of PHB by AR, mediated by several interconnected pathways. Regulation occurs at the levels of transcription, translation and post-translation in a spatial as well as temporal manner. Such intricate regulation is vital for such a ubiquitous protein with many fundamental cellular roles and proven tumour suppressor capacity. The disregulation of PHB control through increased miR27a may promote carcinogenesis or maintenance of oncogenic phenotype in PCa.

Materials and Methods

Mammalian Cell Culture

Cells were maintained at 37˚C in 5% CO_2. HeLa and Cos-1 cells were maintained in Dulbecco's Modified Eagle's Medium (DMEM) [Sigma], LNCaP, DuCaP, VCaP, C42, DU145, PC3 and PC3wtAR cells were maintained in RPMI-1640 (Sigma). All media were supplemented with 10% fetal bovine serum (FBS), 100U/ml penicillin, 100µg/ml streptomycin and 2mM L-glutamine (Sigma). 24-48h prior to ligand treatment, media were replaced with phenol red-free DMEM or RPMI-1640 as appropriate, supplemented with 5% charcoal-stripped FBS, 100U/ml penicillin, 100mg/ml streptomycin and 2mM L-glutamine. RWPE-1 cells were maintained in Keratinocyte-SFM (Life Technologies) supplemented with Epidermal Growth Factor 1-53 (5ng/ml) and Bovine Pituitary Extract (50µg/ml).

Stably transfected LNCaP cell variants - LNCaP/AR-shRNA, LNCaP/scrambled-shRNA (44) were maintained as above with 2.5µg/ml blasticidin, 1ug/ml puromycin. LNCaP/TR2/p2TetR/miR-27a and LNCaP/TR2/pcDNA4/TO-GFP-PHB were generated by stable transfection of LNCaP/TR2 cells (14) with p2TetR-miR-27a and pcDNA4/TO-GFP-PHB respectively, and were maintained as above with 12µg/ml blasticidin, and 300µg/ml zeocin.

Cell Lysis and Protein Extraction

Cells were lysed and protein extracted as described (14). Lysates were stored at -20˚C. See Supp Exp Procedures.

Western Blot Analysis

Proteins were resolved by 8-12% SDS-polyacrylamide gel electrophoresis and electroblotted to nitrocellulose membrane (Bio-Rad). After blocking (5% non-fat dried milk powder in 0.05% Tween-20 in 1x TBS) for 40 minutes, membrane was incubated with mouse anti-AR mAb (Dako, 1/1000), mouse anti-PHB mAb (Neomarkers, 1/1000), or mouse anti-β-actin mAb (Abcam, 1/10,000) for 1h and visualised using goat anti-mouse IgG-HRP. Detection was by ECL reagents (Amersham).

RNA Extraction and Non-Radioactive MiR Northern Blotting

Total RNA was extracted from cells using Trizol reagent (Invitrogen) according to manufacturer's protocol. Northern Blotting was performed on 5-20µg total RNA using double digoxygenin-labelled, LNA-modified probe (Exiqon) complementary to the sequence of mature miR-27a, as described previously (55) with the following amendments: RNA was electrotransferred to positive nylon membrane (Roche) at 300mA for 40 minutes and hybridisation was performed at 37˚C using UltraHyb hybridisation buffer (Ambion), followed by washing in 2xSSC, 0.1% SDS and then 0.1xSSC, 0.1% SDS at 37˚C. Ethidium bromide staining of rRNAs was used as a loading control. Blots were analysed by addition of CDP-Star (Roche) and exposure of film to membrane or by membrane staining with BCIP/NBT (Vector Laboratories). Quantification was performed using Image J software.

Semi-Quantitative RT-PCR

500ng total RNA was reverse transcribed using oligo d(T) primers and the qScript Reverse Transcription kit (PrimerDesign). PCR was performed using 12.5µl TaqReddy Mix (Abgene), 0-2µg cDNA and 25pmol forward and reverse primers per reaction and made to 25µl with ddH_2O. Primer sequences for amplification of PHB 3'UTR, AR, and L19 are

shown (Table 1, Supp Exp Procedures). Samples were thermocycled as follows: 94˚C–4min, 30-40 cycles of (94˚C-30s, 52-65˚C–30-60s, 72˚C–30-120s), 72˚C–10min. PCR products were analysed by agarose gel electrophoresis.

MiR and mRNA Quantification by Quantitative Real-Time RT-PCR

Mature miR expression was quantified by quantitative real-time RT-PCR using the TaqMan microRNA assay for hsa-miR-27a, hsa-miR-23a, hsa-miR-24, hsa-U18 and hsa-miR-182 (Applied Biosystems) and TaqMan Universal PCR Master Mix (Applied Biosystems) according to the manufacturer's protocol. 5-10ng total RNA was reverse transcribed per reaction. PCR was performed using 1.5µl of the obtained cDNA in an ABI 900HT Real-Time PCR System under the 9600 Emulation mode. Cycling conditions were: 95˚C–10mins, 40 cycles of (95˚C–15s, 60˚C–60s). For detection of PHB, primiRs, AR and AR target genes, cDNA was prepared from 500ng total RNA using Precision qScript Reverse Transcription kit (PrimerDesign) and oligo d(T) primer. cDNAs were amplified using 2x Fast SYBR Green Master Mix (Applied Biosystems) and 250nM forward and reverse primers (Table 2, Supp Exp Procedures). All data was analysed using the $\Delta\Delta C_t$ method, with U18 and L19 as endogenous references for miR and mRNA levels respectively, using ethanol-treated samples as calibrators.

Oligonucleotide and Plasmid Transfection

MiR-27a anti-sense (ASO), scrambled ASO and miR-27a mimic were synthesised by MWG Eurofins (see Table 3, Supp Exp Procedures). Transfection of miR-27a/ASO was performed using Dharmafect 2 (Dharmacon) on LNCaP cells at 50% confluency. Transfection complexes were added to cells at a final concentration of 0-500nM. After 24h, RNA was extracted. Whole cell lysates were prepared 48h after transfection. For transfection of LNCaP/GFP-PHB with miR-27a for SRB assays, miR-27a and negative control mimics were

purchased from Dharmacon. Mimic transfection was performed using Lipofectamine RNAiMAX (Invitrogen) to give a final mimic concentration of 100nM. Lipofectamine LTX (Invitrogen) was used for transfection of LNCaP/miR-27a cells with pcDNA4/TO-GFP-PHB to yield final plasmid concentrations of 0.3 or 1.5ng/µl.

PHB-3'UTR Analysis

The 200bp SV40 promoter mRNA sequence was inserted into the MCS of pGL4.18 vector (Promega) using *Bgl*II and *Hind*III restriction sites to generate pSV40-GL4.18. A 900bp DNA fragment corresponding to the PHB-3'UTR was then inserted 3' of the *luc2* gene using *XbaI* and *SalI* to generate the pSV40-GL4.18-PHB-3'UTR vector. Subsequently, miR-27a binding site residues of the 3'UTR were mutated using the QuikChange Lightning Site-Directed Mutagenesis Kit (Stratagene) to produce pSV40-GL4.18-PHB-3'UTR mutant (Fig 2A). pSV40-GL4.18-PHB-3'UTR or the mutant derivative vector (0-8µg) were contransfected with pSVAR and pdmLacZ into HeLa cells using the calcium phosphate method (56). For inhibition of miR-27a activity, miR-27a anti-sense (0-10µg) was transfected into HeLa cells alongside expression and reporter vectors. 24h post-transfection, cells were treated with MB or vehicle (EtOH) and harvested after a further 24h.

PrimiR-23a27a24-2-Specific Drosha Cleavage Activity Assay

The 602bp CMV promoter mRNA sequence was inserted into the MCS of pGL4.18 vector (Promega) using *Nhe*I and *Kpn*I restriction sites to generate pCMV-GL4.18. The 390bp miR-23a27a24-2 genomic sequence was then inserted 5' of the *luc2p* gene and 3' of the CMV promoter in the pCMV-GL4.18 using *Bgl*II and *Hind*III restriction sites to generate the pCMV-primiR-23a27a24-2-GL4.18. This vector was cotransfected into Cos-1 cells alongside

pSVAR and pdmLacZ using the calcium phosphate method (56). 24h post-transfection, cells were treated with MB ± Bic, or vehicle (EtOH) and harvested after a further 24h.

Reporter Assays

Luciferase assays were performed using the Luclite assay (Packard, USA) and activity normalised for transfection efficiency using the Galacton kit (Tropix) as previously described (12). See Supp Exp Procedures.

Chromatin Immunoprecipitations (ChIP)

Cells grown in starvation medium for 3 days were treated with 10nM MB for 0-2 hours. ChIP was performed on formaldehyde cross-linked cell samples as described (57). The presence of miR-23a27a24-2 promoter in immunoprecipitates was quantified by qRT-PCR using 5µl DNA and Fast SYBR Green qPCR mix (Applied Biosystems). Primers shown in Table 4, Supp Exp Procedures.

Sulphorhodamine B (SRB) Assay

Cell number was estimated using the SRB assay as previously described (13). See Supp Exp Procedures.

Statistical Analyses

Normally distributed continuous variables were assessed by student's *t* test. Strength of correlation between two normally distributed continuous variables was assessed by Pearson's correlation coefficient (r). $P \leq 0.05$ was interpreted to denote statistical significance.

Acknowledgements

We thank Professor Malcolm Parker and Dr Nick Dibb for critical reading of the manuscript, and members of the Androgen Signalling Laboratory for technical assistance and helpful discussions. This work was supported by the Medical Research Council of the United Kingdom, Cancer Research UK and The Prostate Cancer Charity.

Conflict of Interest Statement

The authors declare no conflicts of interest in relation to this article.

References

1. Jemal, A., Siegel, R., Xu, J. and Ward, E. (2010) Cancer Statistics, 2010. *CA: Cancer J. Clin.,* **60,** 277-300.
2. Koivisto, P., Kolmer, M., Visakorpi, T. and Kallioniemi, O. (1998) Androgen receptor gene and hormonal therapy failure of prostate cancer. *Am. J. Pathol.,* **152,** 1-9.
3. Chakravarti, D., LaMorte, V.J., Nelson, M.C., Nakajima, T., Schulman, I.G., Juguilon, H., Montminy, M. and Evans, R.M. (1996) Role of CBP/P300 in nuclear receptor signalling. *Nature,* **383,** 99-103.
4. Li, J., O'Malley, B.W. and Wong, J. (2000) p300 Requires Its Histone Acetyltransferase Activity and SRC-1 Interaction Domain To Facilitate Thyroid Hormone Receptor Activation in Chromatin. *Mol. Cell. Biol.,* **20,** 2031-2042.
5. Spencer, T.E., Jenster, G., Burcin, M.M., Allis, C.D., Zhou, J., Mizzen, C.A., McKenna, N.J., Onate, S.A., Tsai, S.Y., Tsai, M.-J. *et al.* (1997) Steroid receptor coactivator-1 is a histone acetyltransferase. *Nature,* **389,** 194-198.
6. Liao, G., Chen, L.-Y., Zhang, A., Godavarthy, A., Xia, F., Ghosh, J.C., Li, H. and Chen, J.D. (2003) Regulation of Androgen Receptor Activity by the Nuclear Receptor Corepressor SMRT. *J. Biol. Chem.,* **278,** 5052-5061.
7. Hodgson, M.C., Astapova, I., Cheng, S., Lee, L.J., Verhoeven, M.C., Choi, E., Balk, S.P. and Hollenberg, A.N. (2005) The Androgen Receptor Recruits Nuclear Receptor CoRepressor (N-CoR) in the Presence of Mifepristone via Its N and C Termini Revealing a Novel Molecular Mechanism for Androgen Receptor Antagonists. *J. Biol. Chem.,* **280,** 6511-6519.
8. Shenouda, S. and Alahari, S. (2009) MicroRNA function in cancer: oncogene or a tumor suppressor? *Cancer Metast. Rev.,* **28,** 369-378.

9. Volinia, S., Calin, G.A., Liu, C.-G., Ambs, S., Cimmino, A., Petrocca, F., Visone, R., Iorio, M., Roldo, C., Ferracin, M. *et al.* (2006) A microRNA expression signature of human solid tumors defines cancer gene targets *Proc. Natl. Acad. Sci. U. S. A.,* **103** 2257-2261

10. Pang, Y., Young, C.Y.F. and Yuan, H. (2010) MicroRNAs and prostate cancer. *Acta Bioch. Bioph. Sin. ,* **42** 363-369

11. Porkka, K.P., Pfeiffer, M.J., Waltering, K.K., Vessella, R.L., Tammela, T.L.J. and Visakorpi, T. (2007) MicroRNA Expression Profiling in Prostate Cancer. *Cancer Res.,* **67,** 6130-6135.

12. Gamble, S.C., Chotai, D., Odontiadis, M., Dart, D.A., Brooke, G.N., Powell, S.M., Reebye, V., Varela-Carver, A., Kawano, Y., Waxman, J. *et al.* (2006) Prohibitin, a protein downregulated by androgens, represses androgen receptor activity. *Oncogene,* **26,** 1757-1768.

13. Gamble, S.C., Odontiadis, M., Waxman, J., Westbrook, J.A., Dunn, M.J., Wait, R., Lam, E.W.F. and Bevan, C.L. (2004) Androgens target prohibitin to regulate proliferation of prostate cancer cells. *Oncogene,* **23,** 2996-3004.

14. Dart, D.A., Spencer-Dene, B., Gamble, S.C., Waxman, J. and Bevan, C.L. (2009) Manipulating prohibitin levels provides evidence for an in vivo role in androgen regulation of prostate tumours. *Endocr. Relat. Cancer,* **16,** 1157-1169.

15. Coates, P.J., Jamieson, D.J., Smart, K., Prescott, A.R. and Hall, P.A. (1997) The prohibitin family of mitochondrial proteins regulate replicative lifespan. *Curr. Biol.,* **7,** 607-610.

16. Steglich, G., Neupert, W. and Langer, T. (1999) Prohibitins Regulate Membrane Protein Degradation by the m-AAA Protease in Mitochondria. *Mol. Cell. Biol.,* **19,** 3435-3442.

17. Mishra, S., Murphy, L.C. and Murphy, L.J. (2006) The Prohibitins: emerging roles in diverse functions. *J. Cell. Mol. Med.,* **10,** 353-363.

18. Wang, S., Fusaro, G., Padmanabhan, J. and Chellappan, S. (2002) Prohibitin co-localizes with Rb in the nucleus and recruits N-CoR and HDAC1 for transcriptional repression. *Oncogene,* **21,** 9.

19. Terashima, M., Kim, K., Adachi, T., Nielsen, P., Reth, M., Kohler, G. and Lamers, M. (1994) The IgM antigen receptor of B lymphocytes is associated with prohibitin and a prohibitin-related protein. *EMBO J.,* **13**.

20. Fusaro, G., Dasgupta, P., Rastogi, S., Joshi, B. and Chellappan, S. (2003) Prohibitin Induces the Transcriptional Activity of p53 and Is Exported from the Nucleus upon Apoptotic Signaling. *J. Biol. Chem.,* **278,** 47853-47861.

21. Rajalingam, K., Wunder, C., Brinkmann, V., Churin, Y., Hekman, M., Sievers, C., Rapp, U.R. and Rudel, T. (2005) Prohibitin is required for Ras-induced Raf-MEK-ERK activation and epithelial cell migration. *Nat. Cell Biol.,* **7,** 837-843.

22. Zhu, B., Zhai, J., Zhu, H. and Kyprianou, N. (2009) Prohibitin regulates TGF-beta induced apoptosis as a downstream effector of smad-dependent and -independent signaling. *Prostate,* **70,** 17-26.

23. Liu, T., Tang, H., Lang, Y., Liu, M. and Li, X. (2009) MicroRNA-27a functions as an oncogene in gastric adenocarcinoma by targeting prohibitin. *Cancer Lett.,* **273,** 233-242.

24. Calin, G.A. and Croce, C.M. (2006) MicroRNA signatures in human cancers. *Nat. Rev. Cancer,* **6,** 857-866.

25. Esquela-Kerscher, A. and Slack, F.J. (2006) Oncomirs - microRNAs with a role in cancer. *Nat. Rev. Cancer,* **6,** 259-269.

26. Calin, G.A., Sevignani, C., Dumitru, C.D., Hyslop, T., Noch, E., Yendamuri, S., Shimizu, M., Rattan, S., Bullrich, F., Negrini, M. *et al.* (2004) Human microRNA genes are frequently located at fragile sites and genomic regions involved in cancers *Proc. Natl. Acad. Sci. U. S. A.,* **101** 2999-3004

27. Cimmino, A., Calin, G.A., Fabbri, M., Iorio, M.V., Ferracin, M., Shimizu, M., Wojcik, S.E., Aqeilan, R.I., Zupo, S., Dono, M. *et al.* (2005) miR-15 and miR-16 induce apoptosis by targeting BCL2 *Proc. Natl. Acad. Sci. U. S. A.,* **102** 13944-13949

28. Johnson, S.M., Grosshans, H., Shingara, J., Byrom, M., Jarvis, R., Cheng, A., Labourier, E., Reinert, K.L., Brown, D. and Slack, F.J. (2005) RAS Is Regulated by the let-7 MicroRNA Family. *Cell,* **120,** 635-647.

29. Catto, J.W.F., Alcaraz, A., Bjartell, A.S., De Vere White, R., Evans, C.P., Fussel, S., Hamdy, F.C., Kallioniemi, O., Mengual, L., Schlomm, T. *et al.* (2011) MicroRNA in Prostate, Bladder, and Kidney Cancer: A Systematic Review. *Eur. Urol.,* **59,** 671-681.

30. Sevli, S., Uzumcu, A., Solak, M., Ittmann, M. and Ozen, M. (2010) The function of microRNAs, small but potent molecules, in human prostate cancer. *Prostate Cancer Prostatic Dis.,* **13,** 208-217.

31. Ozen, M., Creighton, C.J., Ozdemir, M. and Ittmann, M. (2008) Widespread deregulation of microRNA expression in human prostate cancer. *Oncogene,* **27,** 1788-1793.

32. Prueitt, R.L., Yi, M., Hudson, R.S., Wallace, T.A., Howe, T.M., Yfantis, H.G., Lee, D.H., Stephens, R.M., Liu, C.-G., Calin, G.A. *et al.* (2008) Expression of microRNAs and protein-coding genes associated with perineural invasion in prostate cancer. *Prostate,* **68,** 1152-1164.

33. Lee, Y., Kim, M., Han, J., Yeom, K.-H., Lee, S., Baek, S.H. and Kim, V.N. (2004) MicroRNA genes are transcribed by RNA polymerase II. *EMBO J.,* **23,** 4051-4060.

34. Chhabra, R., Dubey, R. and Saini, N. (2010) Cooperative and individualistic functions of the microRNAs in the miR-23a~27a~24-2 cluster and its implication in human diseases. *Mol. Cancer,* **9,** 232.

35. Saini, H.K., Griffiths-Jones, S. and Enright, A.J. (2007) Genomic analysis of human microRNA transcripts *Proc. Natl. Acad. Sci. U. S. A.,* **104** 17719-17724

36. Mi, S., Lu, J., Sun, M., Li, Z., Zhang, H., Neilly, M.B., Wang, Y., Qian, Z., Jin, J., Zhang, Y. *et al.* (2007) MicroRNA expression signatures accurately discriminate acute lymphoblastic leukemia from acute myeloid leukemia. . *Proc. Natl. Acad. Sci. U. S. A.,* **104** 19971-19976

37. Saumet, A., Vetter, G., Bouttier, M., Portales-Casamar, E., Wasserman, W.W., Maurin, T., Mari, B., Barbry, P., Vallar, L., Friederich, E. *et al.* (2009) Transcriptional repression of microRNA genes by PML-RARA increases expression of key cancer proteins in acute promyelocytic leukemia *Blood,* **113** 412-421

38. Mertens-Talcott, S.U., Chintharlapalli, S., Li, X. and Safe, S. (2007) The Oncogenic microRNA-27a Targets Genes That Regulate Specificity Protein Transcription Factors and the G2-M Checkpoint in MDA-MB-231 Breast Cancer Cells. *Cancer Res.,* **67,** 11001-11011.

39. Xi, Y., Formentini, A., Chien, M., Weir, D.B., Russo, J.J., Ju, J., Kornmann, M. and Ju, J. (2007) Prognostic Values of microRNAs in Colorectal Cancer. *Biomark. Insights,* **2006,** 113.

40. Huang, S., He, X., Ding, J., Liang, L., Zhao, Y., Zhang, Z., Yao, X., Pan, Z., Zhang, P., Li, J. *et al.* (2008) Upregulation of miR-23a27a24 decreases transforming growth factor-beta-induced tumor-suppressive activities in human hepatocellular carcinoma cells. *Int. J. Cancer,* **123,** 972-978.

41. Nam, E.J., Yoon, H., Kim, S.W., Kim, H., Kim, Y.T., Kim, J.H., Kim, J.W. and Kim, S. (2008) MicroRNA Expression Profiles in Serous Ovarian Carcinoma *Clin. Cancer Res. ,* **14** 2690-2695

42. Chhabra, R., Adlakha, Y.K., Hariharan, M., Scaria, V. and Saini, N. (2009) Upregulation of miR-23a~27a~24-2 Cluster Induces Caspase-Dependent and -Independent Apoptosis in Human Embryonic Kidney Cells. *PLoS ONE,* **4,** e5848.

43. Buck, A.H., Perot, J., Chisholm, M.A., Kumar, D.S., Tuddenham, L., Cognat, V., Marcinowski, L., Dalken, L. and Pfeffer, S. (2010) Post-transcriptional regulation of miR-27 in murine cytomegalovirus infection *RNA,* **16** 307-315

44. Cheng, H., Snoek, R., Ghaidi, F., Cox, M.E. and Rennie, P.S. (2006) Short Hairpin RNA Knockdown of the Androgen Receptor Attenuates Ligand-Independent Activation and Delays Tumor Progression. *Cancer Res.,* **66,** 10613-10620.

45. Peterziel, H., Mink, S., Schonert, A., Becker, M., Klocker, H. and Cato, A. (1999) Rapid signalling by androgen receptor in prostate cancer cells. *Oncogene,* **18,** 6322-6329.

46. Lee, Y. and Kim, V.N. (2007) In vitro and in vivo assays for the activity of Drosha complex. *Methods Enzymol.,* **427,** 89-106.

47. Zeng, Y. and Cullen, B.R. (2003) Sequence requirements for micro RNA processing and function in human cells. *RNA,* **9,** 112-123.

48. Zeng, Y., Yi, R. and Cullen, B.R. (2005) Recognition and cleavage of primary microRNA precursors by the nuclear processing enzyme Drosha. *EMBO J.,* **24,** 138-148.

49. Jupe, E., Liu, X., Kiehlbauch, J., McClung, J. and Dell'Orco, R. (1996) Prohibitin in breast cancer cell lines: loss of antiproliferative activity is linked to 3' untranslated region mutations. *Cell Growth Differ.,* **7,** 871-878.

50. Sato, T., Saito, H., Swensen, J., Olifant, A., Wood, C., Danner, D., Sakamoto, T., Takita, K., Kasumi, F., Miki, Y. *et al.* (1992) The Human Prohibitin Gene Located on Chromosome 17q21 Is Mutated in Sporadic Breast Cancer. *Cancer Res.,* **52,** 1643-1646.

51. Jakubowska, A., Gronwald, J., Górski, B., Huzarski, T., Byrski, T., Benner, A., Lubiński, J., Scott, R.J. and Hamann, U. (2007) The 3′ untranslated region C > T polymorphism of prohibitin is a breast cancer risk modifier in Polish women carrying a BRCA1 mutation. *Breast Cancer Res. Treat.,* **104,** 67-74.

52. Li, X., Mertens-Talcott, S.U., Zhang, S., Kim, K., Ball, J. and Safe, S. (2010) MicroRNA-27a Indirectly Regulates Estrogen Receptor α Expression and Hormone Responsiveness in MCF-7 Breast Cancer Cells. *Endocrinology,* **151,** 2462-2473.

53. Paik, J.-H., Kollipara, R., Chu, G., Ji, H., Xiao, Y., Ding, Z., Miao, L., Tothova, Z., Horner, J.W., Carrasco, D.R. *et al.* (2007) FoxOs Are Lineage-Restricted Redundant Tumor Suppressors and Regulate Endothelial Cell Homeostasis. *Cell,* **128,** 309-323.

54. Fu, Z. and Tindall, D.J. (2008) FOXOs, cancer and regulation of apoptosis. *Oncogene,* **27,** 2312-2319.

55. Varallyay, E., Burgyan, J. and Havelda, Z. (2008) MicroRNA detection by northern blotting using locked nucleic acid probes. *Nat. Protocols,* **3,** 190-196.

56. Chen, C. and Okayama, H. (1987) High-efficiency transformation of mammalian cells by plasmid DNA. *Mol. Cell. Biol.,* **7,** 2745-2752.

57. Brooke, G.N., Culley, R.L., Dart, D.A., Mann, D.J., Gaughan, L., McCracken, S.R., Robson, C.N., Spencer-Dene, B., Gamble, S.C., Powell, S.M. *et al.* (2011) FUS/TLS Is a Novel Mediator of Androgen-Dependent Cell-Cycle Progression and Prostate Cancer Growth. *Cancer Res.,* **71,** 914-924.

Figure Legends

Figure 1. Androgen signalling downregulates PHB 3'UTR activity. (**A**) Luciferase activity in extracts of HeLa cells cotransfected with wild-type AR expression construct pSVAR and 1µg SV40-GL4-PHB3'UTR prior to 24h treatment with 10nM Mibolerone (MB) vehicle (EtOH). Luciferase was normalised for transfection efficiency (β-galactosidase activity) and mean ± SEM of three independent experiments is shown. (**B**) RT-PCR analysis of PHB-3'UTR, AR and L19 levels in LNCaP/TR2/Scram and LNCaP/TR2/AR shRNA cells treated with doxycycline (dox) for 48h to induce expression of scrambled AR shRNA or AR shRNA. Western blotting was performed on protein lysates to confirm silencing of AR, for which β-actin was used as a loading control. (**C**) *q*RT-PCR analysis of PHB coding region and PHB-3'UTR from PC3wtAR cells treated with MB (10nM) for 24h prior to RNA extraction. Reverse transcription and qPCR were performed using primers as indicated. *Columns:* mean relative gene expression from three independent experiments ± SEM. (**D**) Semi-quantitative RT-PCR analysis of LNCaP cells treated with MB (1nM) ± bicalutamide (Bic) (10µM) for 24h. $P \leq 0.05$, ** $P \leq 0.005$. See also Fig S1.

Figure 2. PHB is a target of MiR-27a Activity in Prostate Cancer Cells. (**A**) Schematic representation of miR-27a binding to PHB 3'UTR and PHB 3'UTR mutant reporter constructs used in (B). See also Fig S2. (**B**) Luciferase reporter activity in extracts from HeLa cells transfected with wild-type AR expression vector pSVAR, 1µg SV40-GL4-Wt/Mutant PHB-3'UTR and 0-5µg p2TetR/miR-27a. Data shown represent mean ± SEM of three independent experiments performed in duplicate. Luciferase activity is normalised for transfection efficiency by cotransfection of β-galactosidase expression vector and data is presented relative to activity of WT reporter in the absence of exogenous miR-7a. (**C**) Western blot analysis of LNCaP/TR2/p2TetR-miR-27a cells treated with 0.0-1.0µM dox for

24h. Image quantification performed using ImageJ software. (**D**) Analysis of relationship between PHB protein levels and miR-27a levels in a panel of prostate cancer cells lines. PHB protein levels were assayed by Western blot and miR-27a levels by qRT-PCR. Data was normalised using β-Actin protein level and U18 expression respectively, and represents mean ± SEM of 3 independent experiments. Pearson correlation coefficient (r) was calculated to assess correlation between PHB protein levels and miR-27a expression. (**E**) qRT-PCR analysis of entire PHB transcript levels from LNCaP/TR2/p2TetR-miR-27a cells treated with dox (0-0.2μM) for 24h to induce miR-27a expression. Data was normalised using L19 expression and represents mean ± SEM of 3 independent experiments performed in triplicate. (**F**) LNCaP cells were transfected with oligos [scrambled (0.2μM), miR-27a (0.2μM), or miR-27a anti-sense (0-1.0μM)]. After 72h, cells were harvested and extracts immunoblotted for β-Actin and PHB protein. Quantification was performed using ImageJ software. Graph shows mean ± SEM of three independent experiments and a representative blot is shown (insert). (**G**) Luciferase reporter activity from HeLa cells transfected with WT SV40-GL4-PHB-3'UTR as for Fig 2B, with the addition of 0-10μg miR-27a ASO. After 48h, cells were harvested, data normalised and presented as for Fig 2B. (**H**) Semi-quantitative RT-PCR analysis of PHB-3'UTR, AR and L19 levels from LNCaP cells transfected with 0.5μg ASO or scrambled oligo. L19 was used as a control for loading and quantification performed using Image J software. Numbers represent relative PHB-3'UTR expression ± SEM. * $P \leq 0.05$, ** $P \leq 0.005$. See also Fig S2.

Figure 3: MiR-27a manipulation alters expression of AR target genes and prostate cancer cell growth. (**A**) qRT-PCR analysis of PSA and TMPRSS2 mRNA levels from LNCaP/TR2/p2TetR-miR-27a cells treated with dox (0-0.2μM) for 24h. L19 expression was used for normalisation of mRNA levels. *Columns:* mean relative mRNA levels from two independent experiments performed in triplicate ± SEM. * $P \leq 0.05$, ** $P \leq 0.05$. (**B,C**)

Sulphorhodamine B growth assays of LNCaP/TR2/p2TetR-miR-27a cells treated with 10nM MB ± 1μM dox to induce miR-27a expression (B) or with additional transfection of GFP-PHB (pcDNA4/TO-GFP-PHB) or empty pcDNA4/TO using Lipofectamine LTX (C). See also Fig S3. (**D**) Sulphorhodamine B growth assays of LNCaP/TR2/pcDNA4/TO-GFP-PHB cells treated with 10nM MB ± 1μM dox to induce GFP-PHB expression, with additional transfection of miR-27a mimic or negative control oligo at a final concentration of 200nM. (**E**) Sulphorhodamine B growth assays of LNCaP cells transfected with miR-27a ASO or a scrambled miR-27a ASO at a final concentration of 50nM ± 10nM MB. (B-E) SRB assays were performed at 0, 2, 4 and 6 days post treatment (B,E) or at 0, 1, 3, 5 and 7 days post transfection/treatment (C,D). *Points:* mean relative absorbance at 492nm, where absorbance at day 0 was set at 1 for all treatment conditions (B,E), absorbance at day 5 in the presence of MB and absence of PHB was set at 1 (C), or absorbance at day 5 in the absence of any treatment was set at 1 (D). Points represent mean of three independent experiments performed in six replicate wells per experiment ± SEM. * $P \leq 0.05$.

Figure 4: The MiR-23a27a24-2 Cluster is Regulated by Androgen in Prostate Cancer Cells. (**A**) qRT-PCR analysis of miR-27a levels from LNCaP cells treated with MB (10nM) or an equal volume of ethanol for 0-24h. RNA was reverse transcribed using miR-specific primers, followed by qPCR for miR-27a. U18 was used as a normalisation gene. (**B**) Diagram illustrating structure of the human miR-23a27a24-2 cluster. (**C**) qRT-PCR analysis of miR-23a27a24-2 cluster members from LNCaP cells treated with MB (1 or 10nM) ± Bic (1 or 10μM) or an equal volume of ethanol for 24h. MiR-specific primers were used for reverse transcription followed by qPCR for mature miR-27a, miR-23a and miR-24 using U18 expression as a normalisation control. *Columns:* mean relative miR expression for three independent experiments performed in triplicate ± SEM. * $P \leq 0.05$, # $P \leq 0.001$ relative to 0h/untreated samples. (**D**) Northern blot analysis of miR-27a levels from 10μg total RNA

extracted from LNCaP cells treated with MB (1 or 10nM) ± Bic (1 or 10μM) or an equal volume of ethanol for 24h. Ethidium bromide staining was performed as a control for equal loading and ImageJ software was used for quantification.

Figure 5: AR Associates with the Proximal Mir23a27a24-2 Promoter in Prostate Cancer Cells in Response to Androgen, Transiently Increasing Primary Transcript Levels and Enhancing Drosha-Mediated PrimiR Cleavage (**A**) Luciferase activity assay of Cos-1 cells transfected with 100ng AR expression vector pSVAR and 1μg of either proximal or distal miR-23a27a24-2 promoter reporter vector for 24h, followed by 24h treatment with MB (10nM) or an equal volume of ethanol. β-galactosidase activity was used as a control for cell number. Data represent mean relative luciferase activity for three independent experiments with duplicate analyses of each RNA sample ± SEM. (**B**) ChIP analysis of AR recruitment to the miR-23a27a24-2 cluster promoter in LNCaP cells treated with MB (10nM) for 0-2h. The purified DNA fraction was probed for presence of proximal miR-23a27a24-2 promoter by qPCR. AR relative enrichment is displayed as a percentage of the input value. Data represent mean AR % pull down relative to IgG for three independent experiments ± SEM. * $P \leq 0.05$. See also Fig S4. (**C**) qRT-PCR analysis of primiR-23a27a24-2 from LNCaP cells treated with MB (10nM) or an equal volume of ethanol for 0-24h. L19 was used as a normalisation gene. Data represent mean of three independent experiments ± SEM. * $P \leq 0.05$, ** $P \leq 0.001$ relative to 0h/untreated samples. See also Fig S5. (**D**) qRT-PCR analysis of primiR-23a27a24-2 and AR levels from LNCaP/Scram and LNCaP/AR shRNA cells treated with dox for 48h to induce expression of scrambled AR shRNA or AR shRNA. L19 expression was used as a normalisation control. (**E**) Luciferase activity in extracts of Cos-1 cells cotransfected with wild-type AR expression construct pSVAR and 100ng CMV-PrimiR-23a27a24-2-GL4 (primiR-23a27a24-2-specific Drosha cleavage reporter) prior to 24h treatment with 1-10nM Mibolerone (MB) ± 1-10μM Bicalutamide (Bic) or vehicle (EtOH).

Luciferase was normalised for transfection efficiency (β-galactosidase activity) and mean ± SEM of three independent experiments is shown. *Upper panel*: diagram illustrating structure of the primiR-23a27a24-2-specific Drosha cleavage reporter. See also See also Fig S6.

Figure 6: Androgen Regulation of the PrimiR-23a27a24-2 Cluster Occurs Post-Transcriptionally. (**A**) qRT-PCR analysis of primiR-23a27a24-2 and mature miR-27a levels (i,ii), or L19 levels (iii) from LNCaP cells grown in stripped medium and treated with Actinomycin D (1μM) and MB (1nM), ethanol, or ethanol or MB (1nM) for 0-48h. Reverse transcription was performed using oligo d(T) primers (primiR-23a27a24-2 and L19) or miR-specific primers (miR-27a). (**B,C,D**) qRT-PCR analysis of miR-23a (B), miR-24 (C) and miR-182 (D) from LNCaP cells grown in stripped medium and treated with Actinomycin D (1μM) ± MB (1nM) for 0-48h. Reverse transcription was performed using miR-specific primers. (A-D) Data represents mean relative gene expression for three independent experiments ± SEM. See also Fig S7. (**E,F**) qRT-PCR analysis of primiR-23a27a24-2 and miR-27a levels from PC3wtAR cells treated with 10nM MB ± 10μM Bic for 24h. L19 and U18 expression levels were used as normalisation controls for primiR-23a27a24-2 and miR-27a levels respectively. Data represent mean ± SEM for three independent experiments. (**G**) qRT-PCR analysis of miR-27a levels from LNCaP/TR2/scram and LNCaP/TR2/AR shRNA cells grown in stripped medium and treated with MB (10nM) ± dox for 48h. U18 expression was used as a normalisation control and data represent mean relative miR-27a expression for three independent experiments ± SEM. * $P \leq 0.05$, ** $P \leq 0.001$.

Figure 7: Model for Androgen and MiR-27a Control of PHB Protein Expression. (1) AR downregulates PHB at the promoter. (2) AR transiently associates with AREs in the miR-23a-27a24-2 promoter, increasing levels of the primary transcript (3) AR enhances primiR to premiR processing (4) In the absence of AR signalling, little primiR is converted to premiR and cellular levels of miR-27a are low (5) PremiR-27a is converted to mature miR-27a by

Dicer in the cytoplasm (6) miR-27a inhibits PHB translation/degrades PHB mRNA. (7) Low PHB leads to increased cell growth. (8) Adding ASO inhibits miR-27a, leading to... (9) Increased cellular levels of PHB. (10) Increased PHB levels inhibit AR activity, which results in...(11) No repression of PHB by AR and (12) No repression of PHB by miR-27a, due to presence of ASO. This results in (13) Further increase in PHB protein levels and ultimately (14) PHB-induced cell cycle arrest.

Abbreviations

ActD	Actinomycin D
AR	Androgen Receptor
ARE	Androgen response element
ASO	Anti-sense oligonucleotide
Bic	Bicalutamide
Dox	Doxycycline
MB	Mibolerone
miR	MicroRNA
miR-27a	*Homo sapiens* microRNA-27a
OncomiR	Oncogenic microRNA
PCa	Prostate cancer
PHB	Prohibitin
PSA	Prostate-specific antigen
shRNA	short hairpin RNA

Figure 1

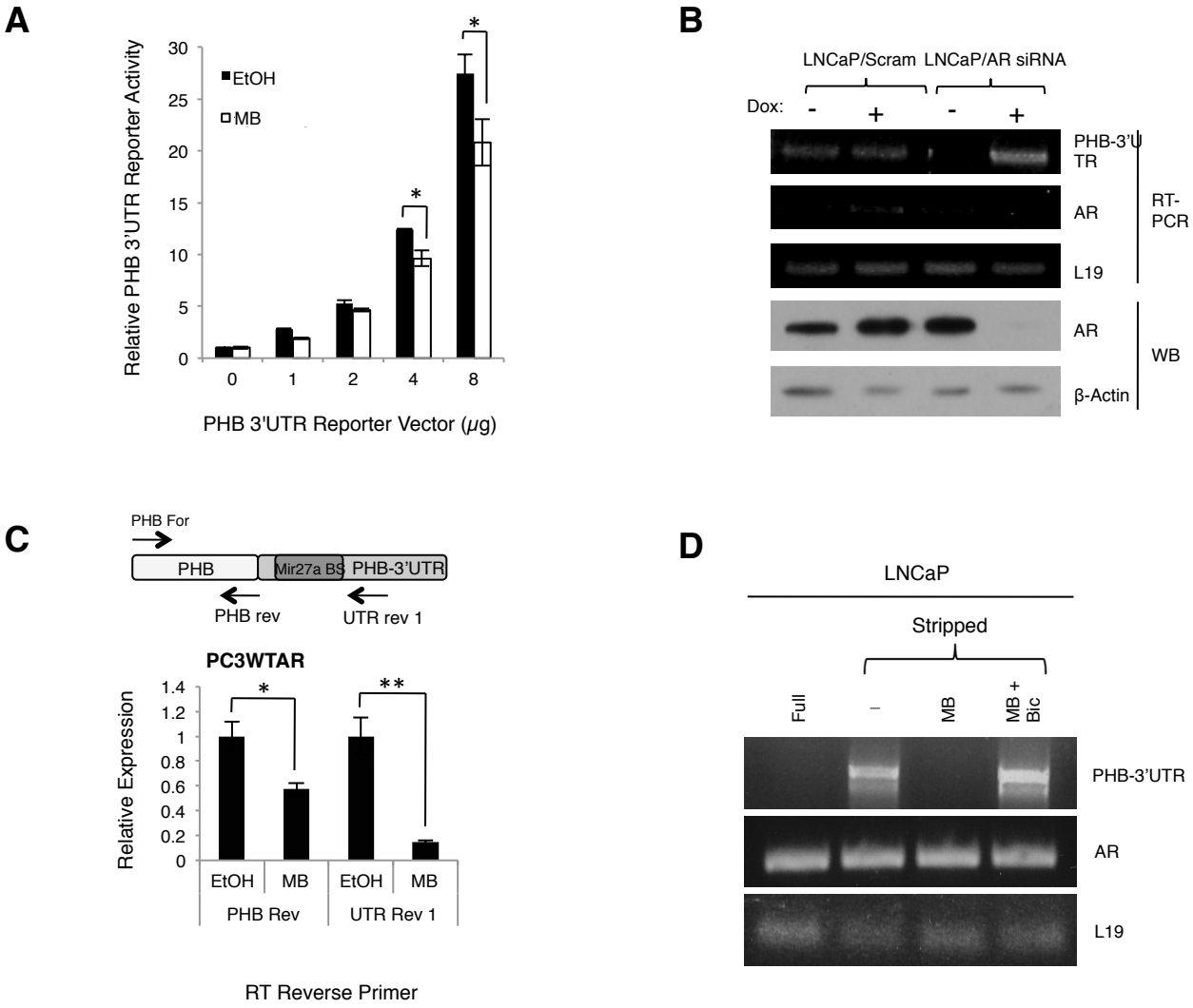
A
Relative PHB 3'UTR Reporter Activity
EtOH
MB
PHB 3'UTR Reporter Vector (μg)
B
LNCaP/Scram
LNCaP/AR siRNA
Dox:
PHB-3'UTR
AR
L19
RT-PCR
AR
β-Actin
WB
C
PHB For
PHB
Mir27a BS
PHB-3'UTR
PHB rev
UTR rev 1
PC3WTAR
Relative Expression
EtOH
MB
PHB Rev
UTR Rev 1
RT Reverse Primer
D
LNCaP
Stripped
Full
–
MB
MB + Bic
PHB-3'UTR
AR
L19

Figure 2

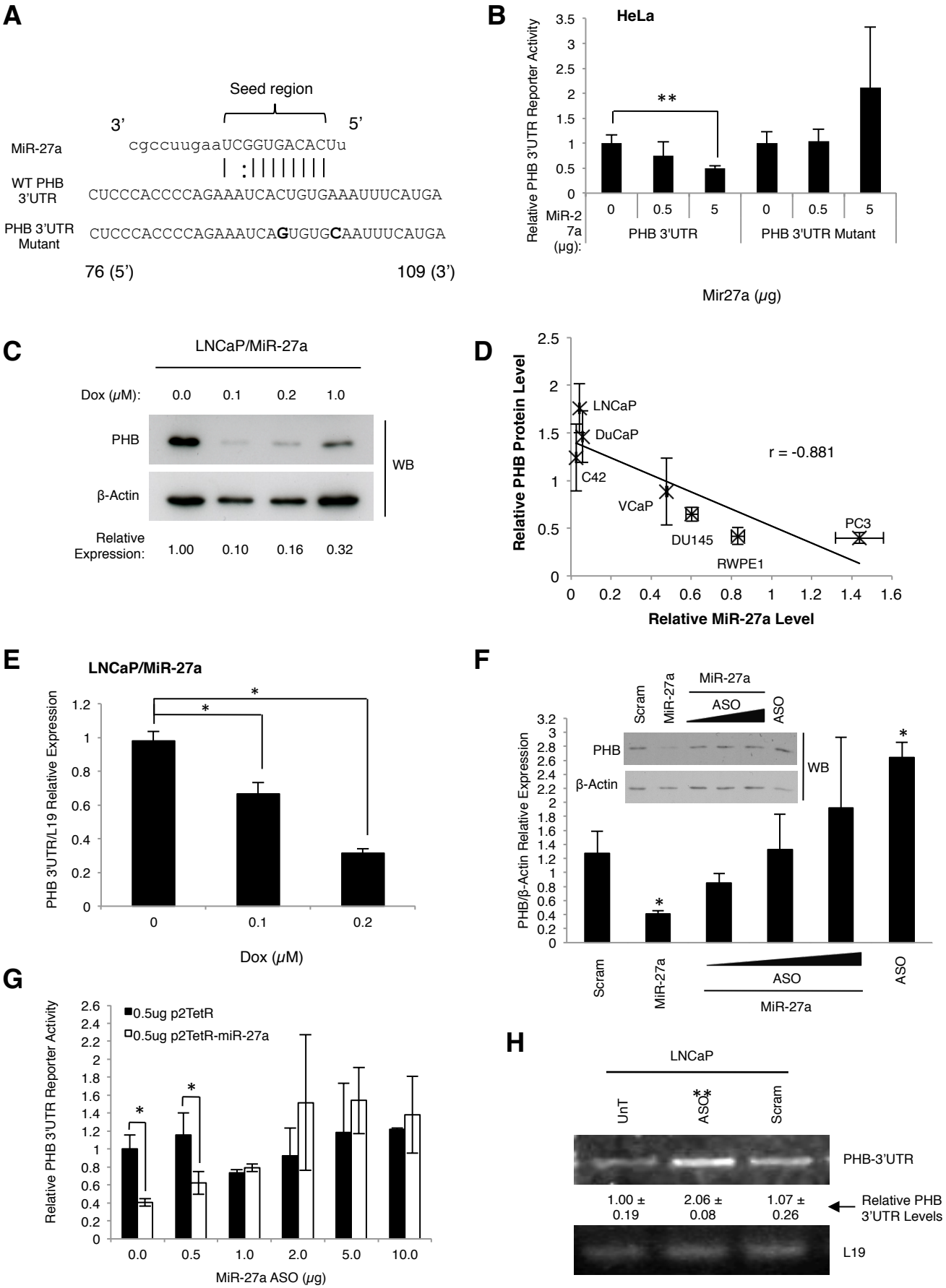
A
Seed region
3'
5'
MiR-27a
cgccuugaaUCGGUGACACUu
WT PHB 3'UTR
CUCCCACCCCAGAAAUCACUGUGAAAUUUCAUGA
PHB 3'UTR Mutant
CUCCCACCCCAGAAAUCAGUGUGCAAUUUCAUGA
76 (5')
109 (3')
B
HeLa
Relative PHB 3'UTR Reporter Activity
MiR-27a (μg):
PHB 3'UTR
PHB 3'UTR Mutant
Mir27a (μg)
C
LNCaP/MiR-27a
Dox (μM):
PHB
β-Actin
WB
Relative Expression:
1.00
0.10
0.16
0.32
D
Relative PHB Protein Level
Relative MiR-27a Level
r = -0.881
LNCaP
DuCaP
C42
VCaP
DU145
RWPE1
PC3
E
LNCaP/MiR-27a
PHB 3'UTR/L19 Relative Expression
Dox (μM)
F
Scram
MiR-27a
ASO
PHB
β-Actin
WB
PHB/β-Actin Relative Expression
G
0.5ug p2TetR
0.5ug p2TetR-miR-27a
Relative PHB 3'UTR Reporter Activity
MiR-27a ASO (μg)
H
LNCaP
UnT
ASO
Scram
PHB-3'UTR
1.00 ± 0.19
2.06 ± 0.08
1.07 ± 0.26
Relative PHB 3'UTR Levels
L19

Figure 3

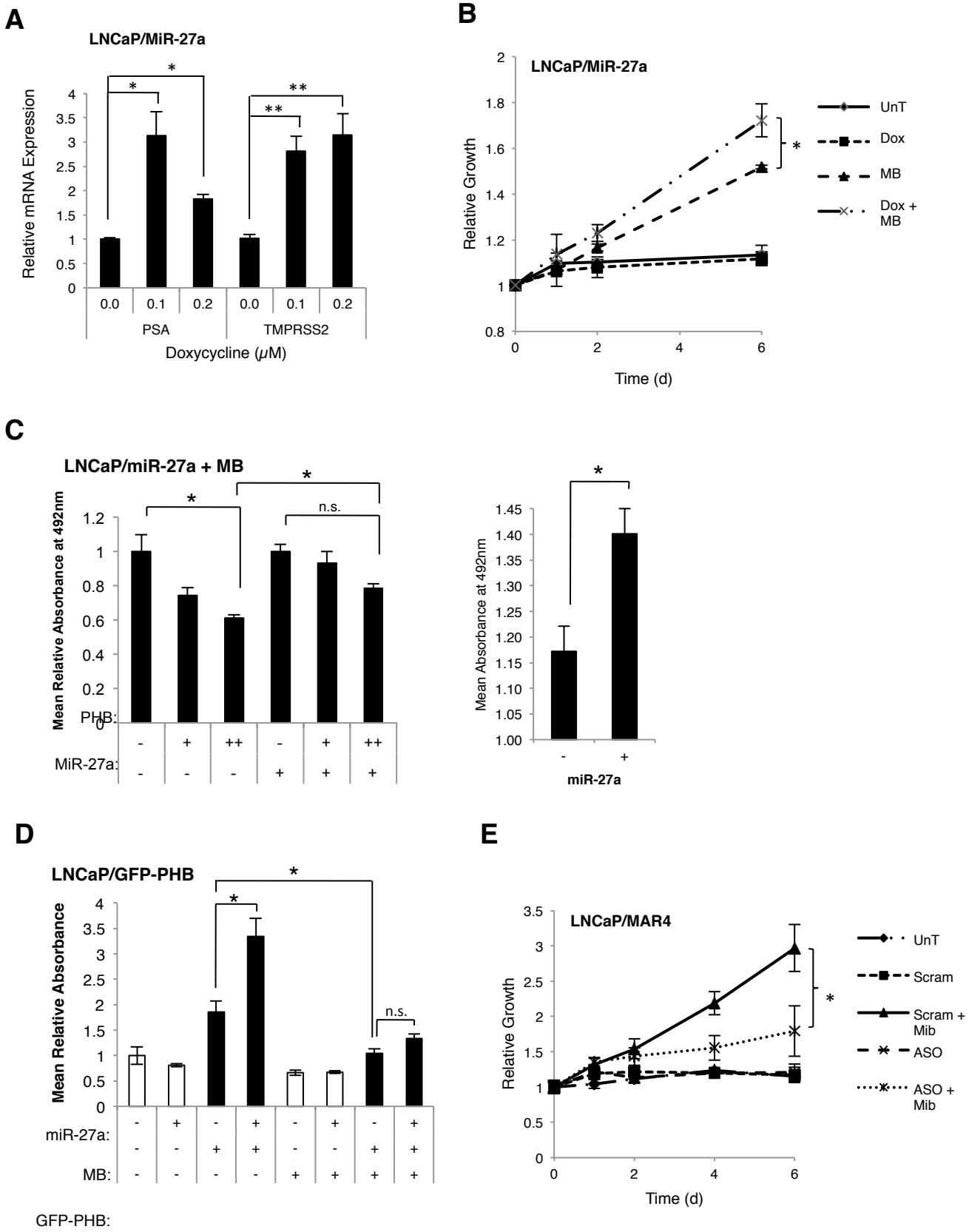
A
LNCaP/MiR-27a
Relative mRNA Expression
Doxycycline (μM)
PSA
TMPRSS2
B
LNCaP/MiR-27a
Relative Growth
Time (d)
UnT
Dox
MB
Dox + MB
C
LNCaP/miR-27a + MB
Mean Relative Absorbance at 492nm
PHB:
MiR-27a:
n.s.
Mean Absorbance at 492nm
miR-27a
D
LNCaP/GFP-PHB
Mean Relative Absorbance
miR-27a:
MB:
GFP-PHB:
E
LNCaP/MAR4
Relative Growth
Time (d)
UnT
Scram
Scram + Mib
ASO
ASO + Mib

Figure 4

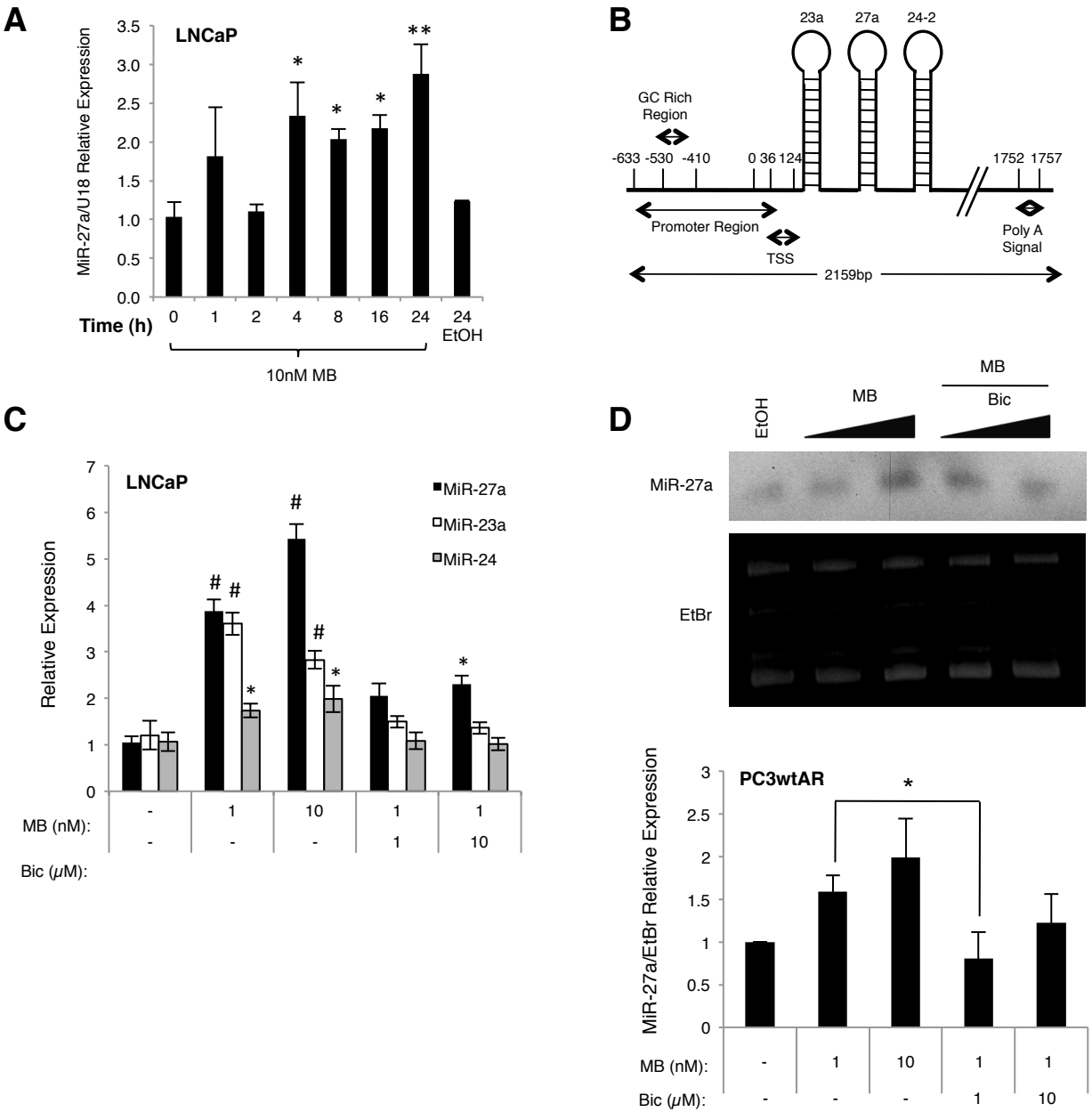
A
LNCaP
MiR-27a/U18 Relative Expression
Time (h)
0 1 2 4 8 16 24 24
EtOH
10nM MB
B
23a
27a
24-2
GC Rich Region
-633 -530 -410
0 36 124
1752 1757
Promoter Region
TSS
Poly A Signal
2159bp
C
LNCaP
MiR-27a
MiR-23a
MiR-24
Relative Expression
MB (nM):
Bic (μM):
D
EtOH
MB
Bic
MiR-27a
EtBr
PC3wtAR
MiR-27a/EtBr Relative Expression
MB (nM):
Bic (μM):

Figure 5

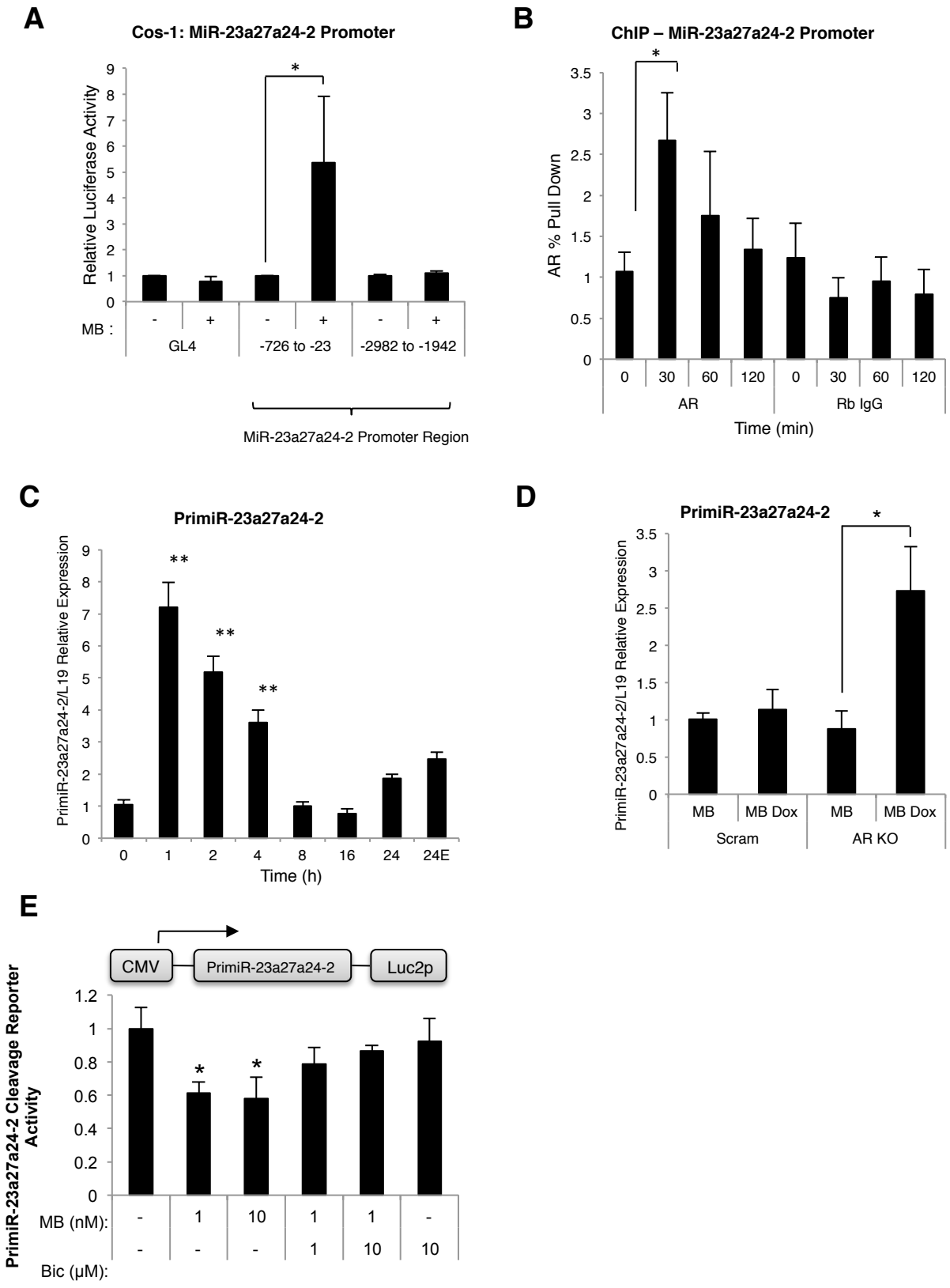
A
Cos-1: MiR-23a27a24-2 Promoter
Relative Luciferase Activity
MB :
GL4
-726 to -23
-2982 to -1942
MiR-23a27a24-2 Promoter Region
B
ChIP – MiR-23a27a24-2 Promoter
AR % Pull Down
AR
Rb IgG
Time (min)
C
PrimiR-23a27a24-2
PrimiR-23a27a24-2/L19 Relative Expression
Time (h)
D
PrimiR-23a27a24-2
PrimiR-23a27a24-2/L19 Relative Expression
MB
MB Dox
Scram
AR KO
E
CMV
PrimiR-23a27a24-2
Luc2p
PrimiR-23a27a24-2 Cleavage Reporter Activity
MB (nM):
Bic (μM):

Figure 6

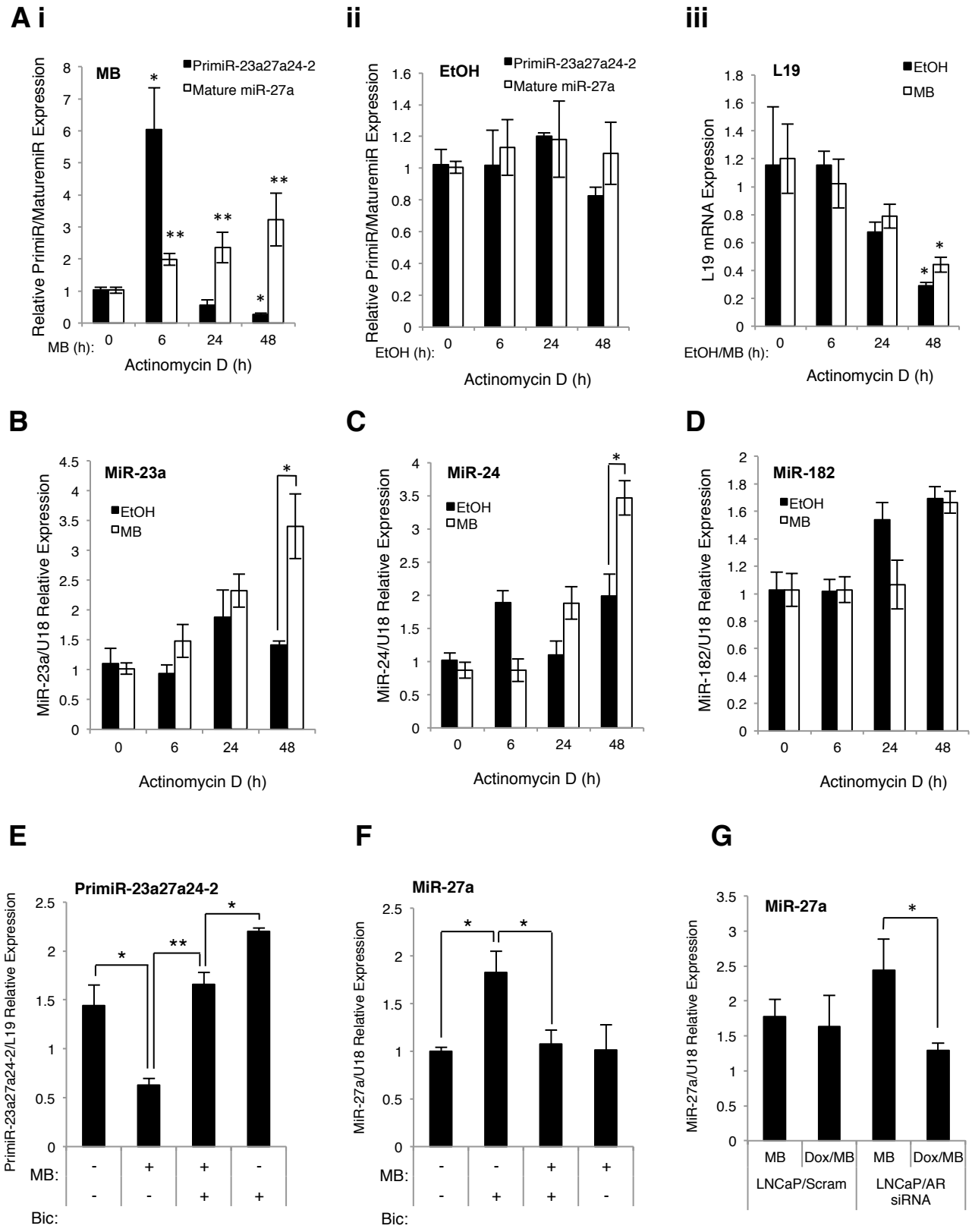
A i
MB
PrimiR-23a27a24-2
Mature miR-27a
Relative PrimiR/MaturemiR Expression
MB (h): 0 6 24 48
Actinomycin D (h)
ii
EtOH
PrimiR-23a27a24-2
Mature miR-27a
Relative PrimiR/MaturemiR Expression
EtOH (h): 0 6 24 48
Actinomycin D (h)
iii
L19
EtOH
MB
L19 mRNA Expression
EtOH/MB (h): 0 6 24 48
Actinomycin D (h)
B
MiR-23a
EtOH
MB
MiR-23a/U18 Relative Expression
0 6 24 48
Actinomycin D (h)
C
MiR-24
EtOH
MB
MiR-24/U18 Relative Expression
0 6 24 48
Actinomycin D (h)
D
MiR-182
EtOH
MB
MiR-182/U18 Relative Expression
0 6 24 48
Actinomycin D (h)
E
PrimiR-23a27a24-2
PrimiR-23a27a24-2/L19 Relative Expression
MB:
Bic:
F
MiR-27a
MiR-27a/U18 Relative Expression
MB:
Bic:
G
MiR-27a
MiR-27a/U18 Relative Expression
MB
Dox/MB
MB
Dox/MB
LNCaP/Scram
LNCaP/AR siRNA

Figure 7

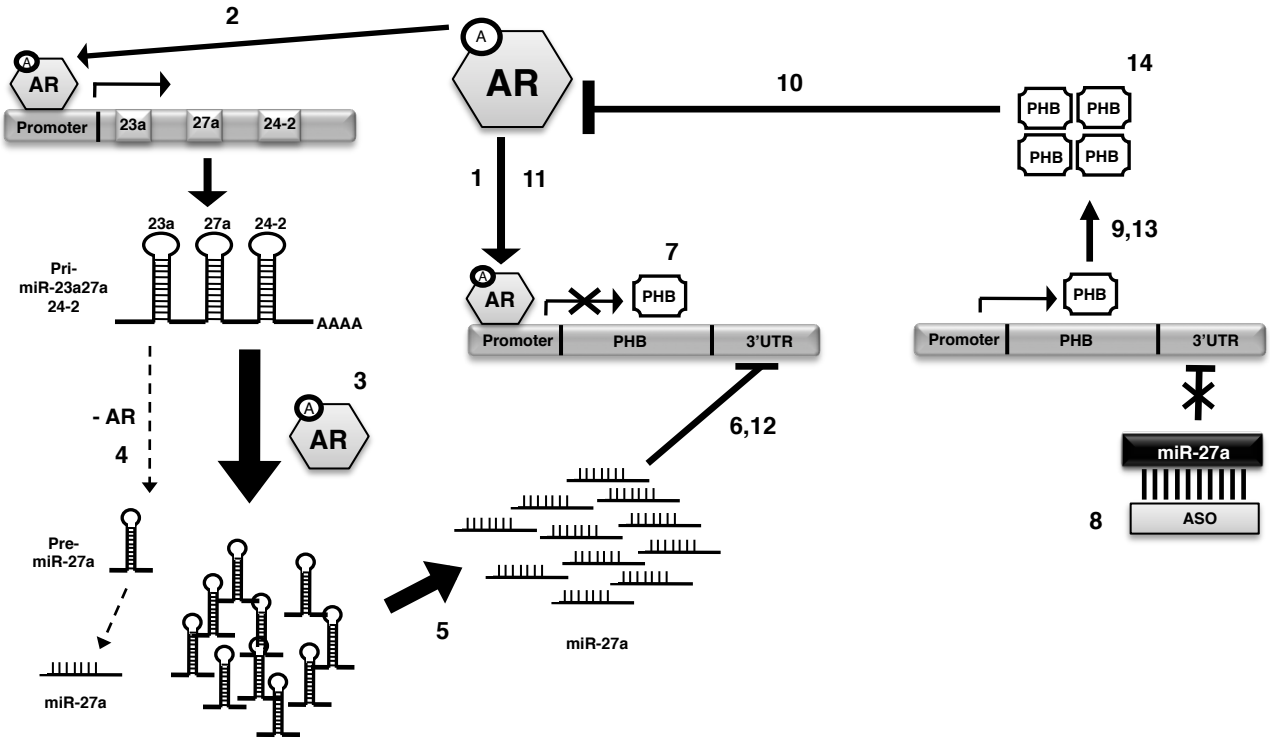
2
AR
Promoter
23a
27a
24-2
1
11
10
14
PHB
PHB
PHB
PHB
9,13
23a
27a
24-2
Pri-
miR-23a27a
24-2
AAAA
7
AR
PHB
Promoter
PHB
3'UTR
Promoter
PHB
3'UTR
3
AR
- AR
4
6,12
miR-27a
ASO
8
Pre-
miR-27a
5
miR-27a
miR-27a

Supplemental Experimental Procedures

Cell Lysis and Protein Extraction

Cells were washed twice with PBS and pelleted by centrifugation at 1000xg for 4 minutes. Pellets were resuspended in cell lysis buffer (100mM NaCl, 0.5% NP40, 50mM Tris-HCl (pH 8.0), 0.2mM PMSF, 5µl/ml proteinase inhibitor cocktail and 10µl/ml phosphatise inhibitor cocktails 1 and 2 [Sigma]). Lysates were incubate on ice for 15min and centrifuged at 13,000xg for 7 minutes to remove cell debris. Supernatant (lysate) was removed and stored at -20˚C.

Luciferase Assay

Luciferase assays were perfomed using the Luclite assay (Packard, USA). Cells frozen in reporter lysis buffer were thawed on ice and 20µl of the lysate was mixed with 20µl of 2x luclite substrate (PerkinElmer) in a 96-well Optiplate (Packard, USA). Plates were incubated at room temperature in the dark for 15 minutes. Luminescence (counts per second) was measured using a VICTOR Light luminescence counter (PerkinElmer). Luminescence values were normalised to β-galactosidase activity (see below).

β-Galactosidase Assay

Assays were performed using the β-galactosidase assay kit (Tropix, UK). Galacton substrate was diluted 100-fold in Galactolight reaction buffer diluent. 5µl of cell lysate was mixed with 50µl of galacton substrate in a 96-well Optiplate. Each plate was incubated for 60 minutes at room temperature in the dark after which 75µl of Accelerator II (Tropix) was added to each well. β-galactosidase activity was measured using the VICTOR Light luminescence counter as described above and used to correct for transfection efficiency.

Sulphorhodamine B (SRB) Assay

Cells were fixed in 100µl (96-well) or 500µl (24-well) 40% trichloroacetic acid (TCA) added directly to cell medium for 1 hour. Plates were washed with water and air-dried. Cells were stained using SRB (0.4%w/v in 1% acetic acid) and incubated for 1 hour. Plates were then washed x5 in 1% acetic acid and air-dried. SRB was solubilised in 100µl (96-well) or 400µl (24-well) 10mM Tris-HCl pH8.0 and absorbance was read at 492nm.

Supplemental Tables

Table 1: Primer Sequences for Semi-Quantitative RT-PCR

Amplification Product	Primers	Primer Sequences
L19	L19 F	5’ GCAGCCGGCGCAAA 3’
	L19 R	5’ GCGGAAGGGTACAGCCAAT 3’
PHB	Prohib F	5’ GGCTGAGCAACAGAAAAAGG 3’
	Prohib R	5’ GCTGGCAGGTAGGTGATGTT 3’
PrimiR-23a27a24-2	Pri23a27a24-2 F	5’-CGCCCGGTGCCCCCCTCACCCCTGTGCCAC-3’
	Pri23a27a24-2R	5’-CCCTGTTCCTGCTGAACTGAGCCAGTGTAC-3’
AR	AR F (E)	5’-CTGCCCCATCCACGTTGTCCCTGCT-3’
	AR R (F)	5’GACTCAGATGCTCCAACGCCTCCAC-3’

Primers Sequences used for Semi-Quantitative RT-PCR. This table relates to Experimental Procedures: Semi Quantitative RT-PCR and Figs **1 and 2**.

Table 2: Primer Sequences for SYBR Green qRT-PCR

Amplification Product	Primers	Primer Sequences
L19	L19 F	5' GCAGCCGGCGCAAA 3'
	L19 R	5' GCGGAAGGGTACAGCCAAT 3'
PHB Coding Region	Prohib F	5' GGCTGAGCAACAGAAAAAGG 3'
	Prohib R	5' GCTGGCAGGTAGGTGATGTT 3'
PHB 3'UTR Full	UTR For	5'-TAATCTAGAGGGCCCACCCTGCCTGCACCTCCGCGGG-3'
	UTR rev long NRS	5'-GGAAGGTCTGGGTGTCATTTATTGACAGCAGTTT-3'
PrimiR-23a27a24-2	Pri23a27a24-2 F	5'-CGCCCGGTGCCCCCCTCACCCCTGTGCCAC-3'
	Pri23a27a24-2R	5'-CCCTGTTCCTGCTGAACTGAGCCAGTGTAC-3'
AR	AR F (E)	5'-CTGCCCCATCCACGTTGTCCCTGCT-3'
	AR R (F)	5'GACTCAGATGCTCCAACGCCTCCAC-3'
TMPRSS 2	TMPRSS2 F	5'-AATCGGTGTGTTCGCCTCTAC-3'
	TMPRSS2 R	5'-GCGGCTGTCACGATCC-3'
PSA	PSA F	5' TTGTCTTCCTCACCCTGTCC 3'
	PSA R	5' AGCTGTGGCTGACCTGAAAT 3'
KLK2	KLK2 F	5' CCTCACGTTCTGGCATCACTT 3'
	KLK2 R	5' CGGCCAGGTGAGTTCCAA 3'
PHB 3'UTR long	PHB for	5' GGCTGAGCAACAGAAAAAGG 3'
	UTR rev 3	5'-ATACAAGTCCATCCAAGTTTTAGGACCCTG-3'
PHB 3'UTR mid	PHB for	5' GGCTGAGCAACAGAAAAAGG 3'
	UTR rev 2	5'-CTCATCCGCAAACCTTCCATCAGTGACAG-3'
PHB 3'UTR short	PHB for	5' GGCTGAGCAACAGAAAAAGG 3'
	UTR rev 1	5'-CTAATTAGAGATCTGAAGTGATTTTACCTT-3'

Primers Sequences used for SYBR Green qRT-PCR. This table relates to Experimental Procedures: MiR and mRNA Quantification by Quantitative Real-Time RT-PCR and **Figs 2, 3, 4, 5, 6, S5 and S7.**

Table 3: MiR Oligonucleotide Sequences for Transfections

Name	Sequence
miR-27a mimic	5’ TTCACAGTGGCTAAGTTCCGC 3’
miR-27a ASO	5’ GCGGAACTTAGCCACTGTGAA 3’
miR-27a ASO scram	5’ TGACCGTATAGGCTAAGCGAC 3’

Oligonucleotide Sequences used for MiR/ASO Transfections. This table relates to Experimental Procedures: Oligonucleotide Transfections and **Fig 2**.

Table 4: Primer Sequences for qPCR Following Chromatin Immunoprecipitation

Name	Sequence
miR prom ChIP for	5'-GCAGGTACCGTGCTGGGCACTTACTGAGTGA-3'
miR prom ChIP rev	5'-GCCACTTCCTAGAAGCCTGGAG-3'

Primers Sequences used for Chromatin ImmunoprecipitationSYBR Green qPCR. This table relates to Experimental Procedures: Chromatin Immunoprecipitation (ChIP) and **Fig 5**.

Supplemental Figure 1

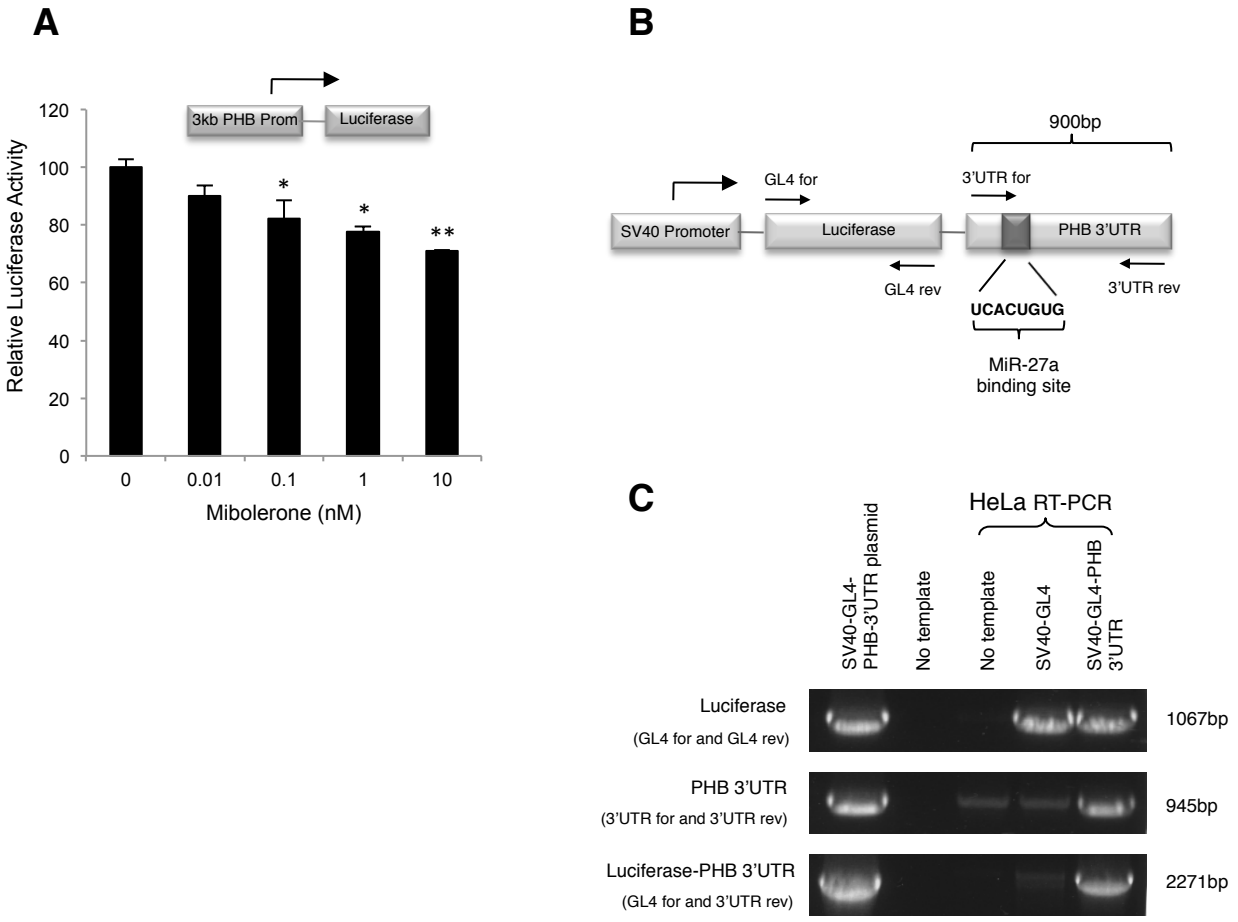

Figure S1: Androgen signalling downregulates PHB promoter activity and Luciferase-PHB 3'UTR is expressed from the SV40 promoter of the SV40-GL4-PHB-3'UTR vector upon transient transfection into HeLa cells. *(A)* Relative luciferase activity was measured in serum-deprived Cos-1 cells co-transfected with 3kb proximal PHB promoter reporter construct and wild-type AR expression vector ± mibolerone (MB) (0-10nM) for 24h. β-galactosidase activity was used as a control for cell number. Data represent mean relative luciferase activity for three independent experiments with duplicate analyses of each RNA sample ± SEM. *(B)* Diagram showing the structure of the SV40-GL4-PHB 3'UTR vector and regions amplified by primers used for RT-PCR. *C)* RT-PCR analysis of luciferase, PHB 3'UTR and luciferase-PHB 3'UTR from RNA from HeLa cells transiently transfected with SV40-GL4 or SV40-GL4-PHB 3'UTR plasmids. * $P \leq 0.05$. These data relate to **Fig 1**.

Supplemental Figure 2

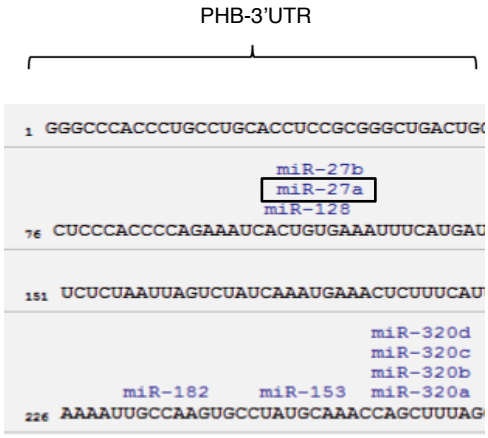

Figure S2: PHB 3'UTR is a predicted target of miR-27a. Diagram illustrating locations of predicted miR associations with the PHB-3'UTR. Data from http://microrna.org. These data relate to **Fig 2**.

Supplemental Figure 3

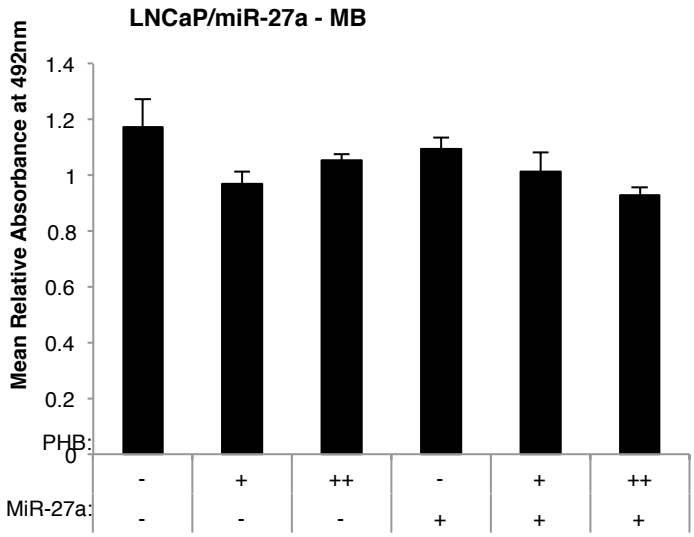

Figure S3: MiR-27a and PHB overexpression do not alter prostate cancer cell growth in the absence of androgen. Sulphorhodamine B growth assays of LNCaP/TR2/p2TetR-miR-27a cells treated with 1μM dox to induce miR-27a expression and transfected with GFP-PHB (pcDNA4/TO-GFP-PHB) or empty pcDNA4/TO using Lipofectamine LTX. SRB assays were performed at 0, 1, 3, 5 and 7 days post-transfection/treatment. *Bars: m*ean relative absorbance at 492nm, where absorbance at day 5 in absence of PHB was set at 1. Data represent mean relative absorbance at 492nm for three independent experiments ± SEM. These data relate to **Fig 3**.

Supplemental Figure 4

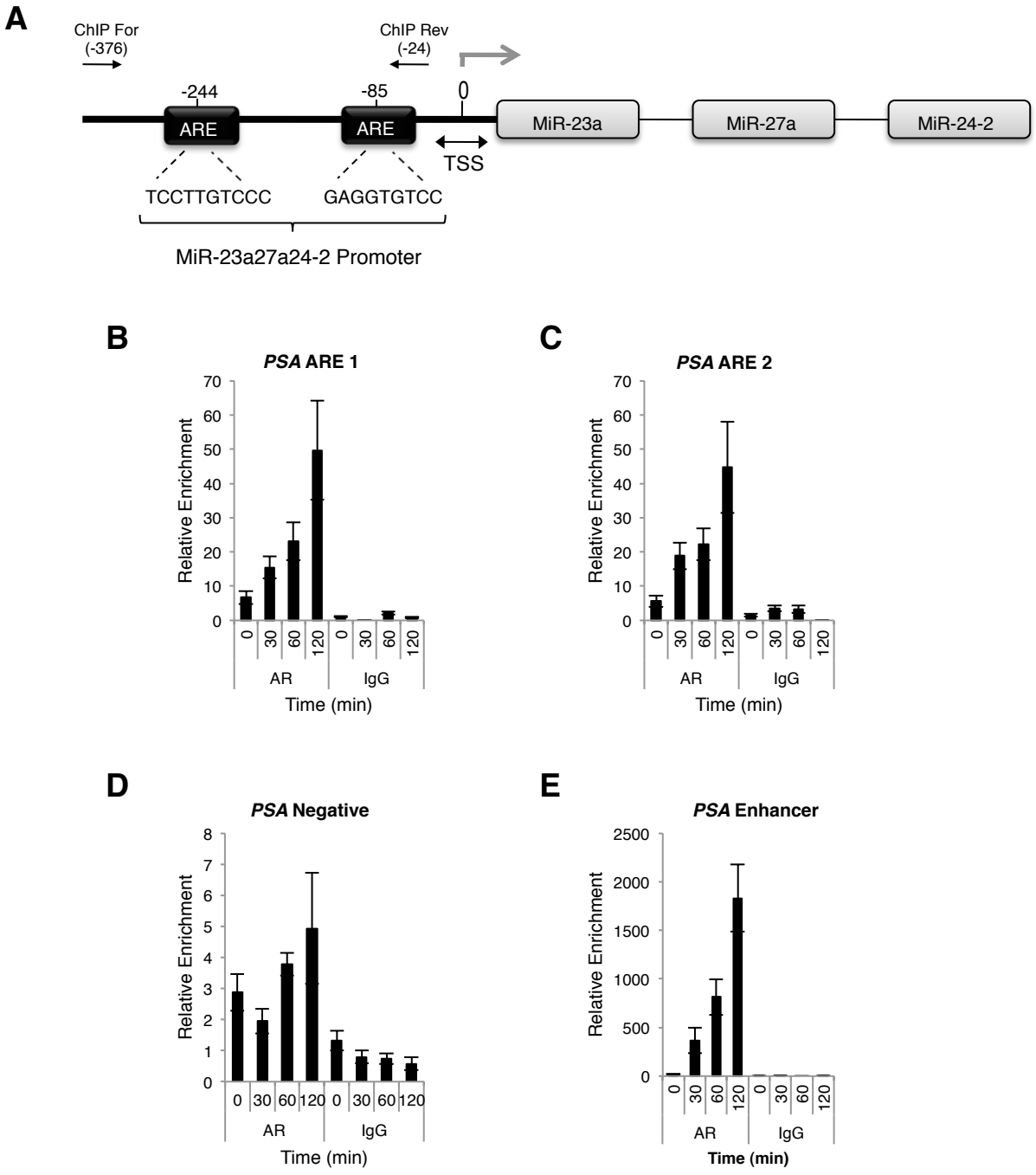

Figure S4: The miR-23a27a24-2 promoter contains putative AREs and AR is recruited to the *PSA* Gene Promoter in the Presence of Androgen. *(A)* Diagram illustrating the location of predicted AREs within the miR-23a27a24-2 proximal promoter. Primers used for chromatin immunoprecipitation are indicated by small black arrows. AREs were predicted using the ALGGEN algorithm (http://alggen.lsi.upc.es/). *(B,C,D,E)* ChIP analysis of AR recruitment to AREs of the *PSA* promoter in LNCaP cells treated with MB (10nM) for 0-2h. The purified DNA fraction was probed for presence of PSA ARE1 *(B)*, PSA ARE2 *(C)*, PSA ARE negative region *(D)* and PSA ARE3 (enhancer) *(E)* by qPCR. AR relative enrichment represents AR recruitment to promoter regions relative to input levels. Data represent mean relative AR enrichment for three independent experiments ± SEM. * $P \leq 0.05$. These data relate to **Fig 5**.

Supplemental Figure 5

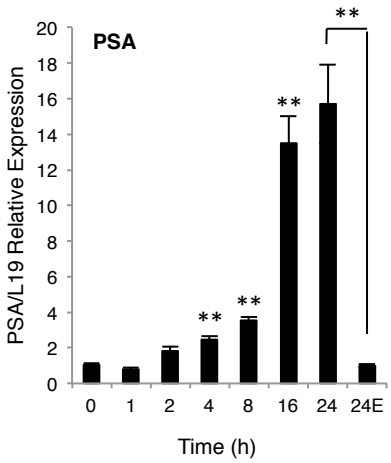

Figure S5: Androgen Treatment Increases Expression of *PSA*. qRT-PCR analysis of *PSA* from LNCaP cells treated with MB (10nM) or an equal volume of ethanol for 0-24h. L19 was used as a normalisation gene. Data represent mean of three independent experiments ± SEM. ** $P \leq 0.001$ relative to 0h/untreated samples. These data relate to **Fig 5**.

Supplemental Figure 6

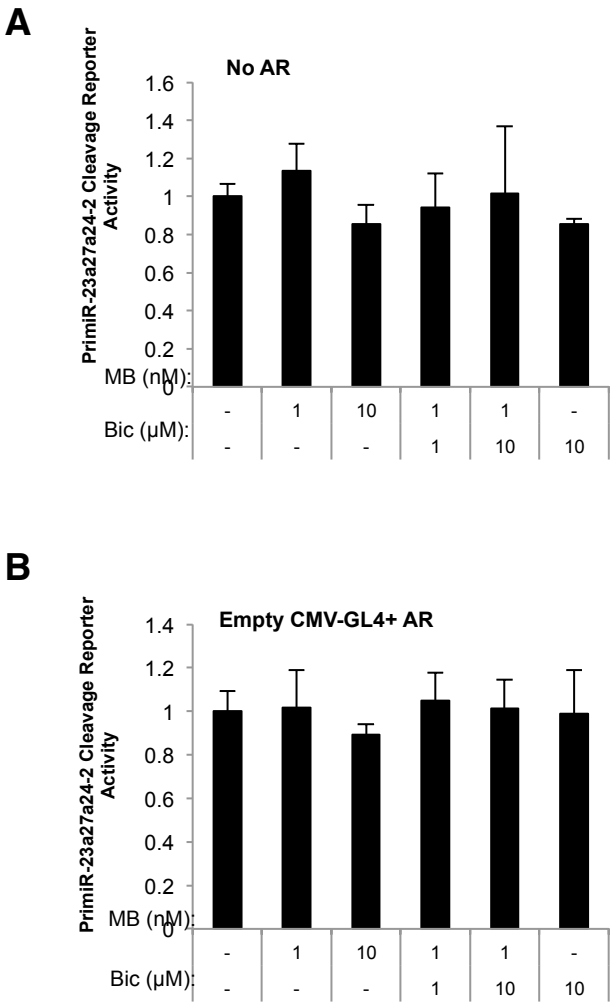

Figure S6: PrimiR-23a27a24-2-specific Drosha reporter activity is not altered in the absence of androgen or in the presence of empty CMV-GL4 vector. Luciferase activity in extracts of Cos-1 cells transfected with either (**A**) 100ng CMV-PrimiR-23a27a24-2-GL4 (primiR-23a27a24-2-specific Drosha cleavage reporter) in the absence of AR, or (**B**) 100ng empty CMV-GL4 vector and wild-type AR expression construct pSVAR, and treated with 1-10nM Mibolerone (MB) ± 1-10μM Bicalutamide (Bic) or vehicle (EtOH) for 24h. Luciferase was normalised for transfection efficiency (β-galactosidase activity) and mean ± SEM of three independent experiments is shown. These data relate to **Fig 5**.

Supplemental Figure 7

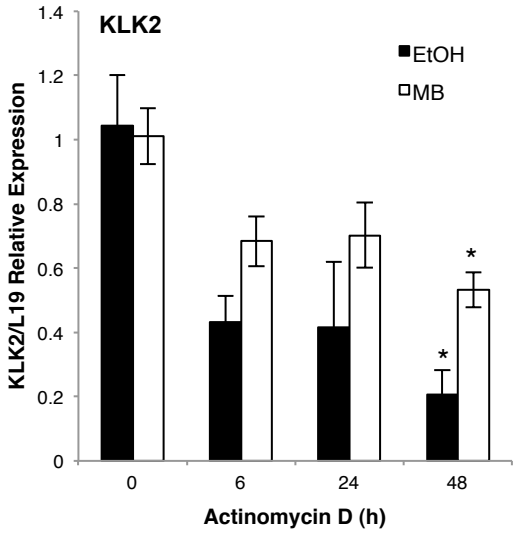

Figure S7. Transcript levels of the androgen-regulated gene, *KLK2*, are reduced in prostate cancer cells treated with actinomycin D ± MB. qRT-PCR analysis of KLK2 levels from LNCaP cells grown in stripped medium and treated with Actinomycin D (1μM) and MB (1nM) or ethanol for 0-48h. Reverse transcription was performed using oligo d(T) primers. Data represents mean relative gene expression for three independent experiments ± SEM. * $P \leq 0.05$. These data relate to **Fig 6.**